



Diagnosing Aerosol-Meteorological Interactions on Snow within the Earth System: A Proof-of-Concept Study over High Mountain Asia

Chayan Roychoudhury¹, Cenlin He², Rajesh Kumar², and Avelino F. Arellano Jr.¹

¹Department of Hydrology and Atmospheric Sciences, University of Arizona, Tucson, AZ, USA

²Research Applications Laboratory, NSF National Center for Atmospheric Research, Boulder, CO, USA

Correspondence: Chayan Roychoudhury (croychoudhury@arizona.edu)

Abstract. Snowmelt in the Third Pole, particularly in High Mountain Asia (HMA), is strongly influenced by interactions between aerosols and meteorology. However, understanding these interactions remains uncertain due to their complexity and limitations in existing approaches using model sensitivity and process-denial experiments. In addition, these interactions are insufficiently represented in current climate models. Equally ambiguous is the impact of these interactions on snow processes in the context of climate change. Here we use network theory to identify key variables that influence non-linear processes within snowmelt using daily data for the late snowmelt season (May-July). We combine statistical and machine learning methods using observational and model data, to highlight the underappreciated relevance of coupled processes between aerosols and meteorology on snow, as well as the inconsistent representation of aerosol-meteorology interactions on snow within major reanalyses, reflective of differences in model design. In particular, dust interactions with near-surface temperature and large-scale circulation are underrepresented, as well as gaps in cloud cover interactions especially in the least coupled reanalysis. Carbonaceous aerosols and large-scale circulation emerge as main drivers of aerosol-meteorology onto snow interactions, highlighting their relevance in Earth system models (ESMs) for the accurate assessment of water availability in developing economies. These diagnoses point to the degree of complexity of these interactions and their relative strength of representation across ESMs. The proposed framework can thus be extended to diagnose other complex Earth system processes, providing a pathway for improving Earth system predictability and reducing climate change uncertainties.

1 Introduction

The rapid acceleration of glacial snowmelt in recent decades has critically impacted the freshwater resources that serve the livelihood of regions downstream of these glaciers (Kraaijenbrink et al., 2021). The negative trends in snow cover fraction (SCF) observed in recent decades pose an imminent risk to the glacial water towers of HMA, spanning the Tibetan Plateau and surrounding mountain ranges in Asia. These trends highlight the susceptibility of HMA to the complex interplay between the land and atmosphere and its cascading effects, impacting snowmelt and ultimately water resources (Mudryk et al., 2020; Barnett et al., 2005). SCF is an essential climate variable that is particularly sensitive to climate change and modulates the surface energy balance and atmospheric circulation (Cohen and Entekhabi, 2001; Cerveny and Balling Jr., 1992). The high albedo of snow leads to feedbacks between the snow surface and the atmosphere where the highly reflective snow surface



25 melts in response to atmospheric warming, exposing the darker underlying surface (thus lowering the albedo). The exposed surface absorbs a greater amount of solar radiation, which enhances atmospheric warming and accelerates snowmelt. These changes in the cryosphere influence the Earth's radiation budget, contributing to the broader Earth system feedbacks that drive climate change (Flanner et al., 2011; Robock, 1983; Hileman, 1992).

Past studies have attributed meteorological factors such as ambient temperature, precipitation, and topography as the primary drivers of variations in SCF within HMA, often overlooking the relevance of anthropogenic emissions in the vicinity of glaciers in driving these feedbacks (Bonekamp et al., 2021; Sorg et al., 2012; Pepin et al., 2015; Singh et al., 2022). Light absorbing particles (LAPs, such as black and brown carbon (BC, BrC), and dust) are a key component of these emissions that have a considerable impact on snow cover through aerosol deposition on snow, with an efficacy comparable to greenhouse gases (Warren and Wiscombe, 1980; Qian et al., 2015; Kang et al., 2020; Shindell and Faluvegi, 2009; Sarangi et al., 2020; Brown et al., 2022; Wang et al., 2023). The interactions between meteorology and aerosols (mostly but not limited to LAPs) onto snow, hereby defined as aerosol-meteorology interactions at the snow interface (AMI) are diverse, ranging from (a) altering the Earth's radiation budget and thereby affecting atmospheric thermodynamics; (b) changing cloud microphysical properties, precipitation rate and type; (c) modifying snow albedo feedbacks by deposition leading to snow darkening; and (d) modifying snow properties such as specific surface area, that further amplify the snow-albedo feedback (ram; He, 2022; Andreae and Rosenfeld, 2008; Painter et al., 2007; Lohmann and Feichter, 2005; Flanner et al., 2007; Huang et al., 2022; Lohmann, 2017; Borys et al., 2000). Additionally, deposition of these LAPs has different sources: BC and BrC are dominated by anthropogenic sources, while dust mostly originates from natural sources in desert regions in the vicinity of HMA (Shi et al., 2019). Combined with the spatial heterogeneity in the glaciers across HMA, the non-linear interaction of these processes can either intensify or buffer the response of the climate system, confounding the net effect of AMI on the cryosphere and misattributing the relevant drivers to snowmelt (Sakai and Fujita, 2017; Ragetti et al., 2016; Kapnick et al., 2014; Bonekamp et al., 2019; Sand et al., 2020; Stevens and Feingold, 2009; Michibata et al., 2020; Gautam et al., 2013; Rahimi et al., 2020). For instance, recent studies place contrasting degrees of importance on the types of LAPs and their radiative impact on snow. Although BC has been the primary candidate of study in aerosol-induced snow albedo feedback within the recent decades, the state of science is constantly changing, and it is realized that dust and BrC are more important than previously thought (Tuccella et al., 2021).

50 An improved understanding of these interacting processes plays a crucial role in accurately predicting climate change, especially freshwater availability in Third Pole regions like the HMA (Zhang et al., 2019). A systems-science approach to resolving these non-linear processes views the Earth's climate as a self-regulating system of organized complexity with feedbacks among its sub-components (Wood Jr, 1988). Current prediction models reflect this, where the scientific community has progressed from simple physical models (considering temperature, humidity, solar insolation, etc.) to fully coupled Earth system models (ESMs) (both regional and global) by incorporating complex feedbacks related to atmospheric composition like the carbon cycle and aerosols (Flato, 2011; Nobre et al., 2010; Giorgi and Gao, 2018). Current state-of-the-art ESMs have only recently been able to incorporate some degree of atmospheric composition feedbacks into coupled atmosphere-ocean models (van Vuuren et al., 2012). These limitations are further complicated by the fact that incorporating additional processes and interactions in ESMs shows an increased uncertainty in projections of various climate variables like surface temperature (Meehl and Zhao,



60 2007; Stainforth et al., 2005), and highlights the gaps in current ESMs to fully simulate these coupled Earth system processes. Therefore, in addition to an improved quantification and accounting of these diverse feedbacks, it is essential to evaluate and assess the performance of current ESMs and coupled regional models to reduce these uncertainties.

Challenges in constraining these non-linear interactions arise from a variety of factors, that include 1) sparsity in long-term continuous observations 2) theoretical uncertainty in parameterization and coupling, 3) spatio-temporal heterogeneity in the processes, and 4) magnitude and direction of these feedbacks. Conventional methods to separate and constrain these uncertainties in coupled ESMs have often been through 1) generating model ensembles by perturbing model parameters and assessing their sensitivities or 2) withholding selected modeled parameters and comparing their relative impacts, 3) using observations and data-assimilation (Schneider et al., 2017), and 4) assessing emergent constraints across multiple models, (Heinze et al., 2019; Soden et al., 2008; Zhou et al., 2019; Moch et al., 2022; Gettelman, 2015; Barthlott et al., 2022; Archer-Nicholls et al., 2016; Usha et al., 2020; Stein and Alpert, 1993). Although valuable, the heavy computational burden of these approaches compels us to investigate other possibilities. Following the systems-science paradigm, Harte (2002) suggests integrating a Newtonian (top-down, system-wide analysis) and Darwinian (bottom-up, process-level analysis) perspective to enhance our understanding of complex Earth system processes and potentially constrain their uncertainties. Simpler statistical techniques ranging from regression to emulators have been suggested to provide a more simplified understanding of these interactions, albeit with their limitations (Carslaw et al., 2013; Johnson et al., 2015; Lee et al., 2013; Xiao et al., 2023; Wall et al., 2022; Gregory et al., 2004). Recent advancements in artificial intelligence for emulating complex systems also provide a viable alternative (Reichstein et al., 2019; Shin et al., 2022; Schneider et al., 2017), although they are often still perceived as black boxes introducing additional complexity and biases (Castelvecchi, 2016; Lipton, 2018). In the domain of aerosol-cloud interactions (ACI), Harte's approach has been proposed to constrain ACI-related feedbacks by a combination of process modeling and observational measurements (Feingold et al., 2016). Thus, a similar approach can be adopted to diagnose these feedbacks at the Earth system interface, where the system-wide complexity is reduced into second-order non-linear interactions between different simpler sub-systems, Our study applies this approach by attempting to diagnose second-order feedbacks between atmospheric composition (particularly aerosols) and meteorology that influence the cryosphere interface, (i.e., snow surface) over High Mountain Asia (HMA), a key region in the Third Pole, which stores significant amounts of freshwater reserves as glaciers outside of the polar regions (Yao et al., 2019).

The lack of consistent geophysical observations across regions like HMA, partly driven by its remoteness and complex terrain, requires the use of reanalysis products such as ERA5/CAMS-EAC4 and MERRA-2 that provide an opportunity for understanding long-term changes in HMA. In a previous study, we attempted to address AMI by quantifying the importance of second-order interactions between aerosol and meteorological variables from ERA5/CAMS-EAC4 reanalysis to satellite-based MODIS SCF using a multi-linear regression model (Roychoudhury et al., 2022). We found that AMI, particularly those related to carbonaceous aerosols, holds high importance for glacial regions with low snow cover (LSC) in HMA, particularly during the late snowmelt season (May-July). Our goal in this study is to assess whether we can diagnose AMI at the snow interface over HMA across three comprehensive reanalyses of varying levels of complexity, and acquire insights into the AMI-related processes captured in each of these reanalyses. As mentioned before, we embrace an integration of the Newtonian-Darwinian



95 perspectives inspired by (Harte, 2002) and attempt to reduce the complexity of the interconnected processes linking snow, aerosols, and meteorology into specific second-order non-linear interactions between aerosols and meteorology onto snow (i.e., AMI) and quantify their significance to SCF variability.

Our definition of AMI has an additional layer of complexity due to its relevance to the cryosphere and the land-atmosphere interface. In contrast to the approach by Feingold et al. (2016) which explores ACI as a product of the sensitivities of different cloud properties to cloud radiative forcing, we instead account for joint dependencies (pairwise/two predictors simultaneously) between aerosol and meteorological drivers of snowmelt through observations and reanalysis data. Previous studies like Usha et al. (2020) and He et al. (2018) are oriented towards the Newtonian perspective, where the sensitivity of snow properties to aerosol parameters are explored, whereas trends and attribution studies as in Sorg et al. (2012) and Pepin et al. (2015) are aligned more towards the Darwinian perspective, where snow related trends are attributed to meteorological and/or topography variables. The missing element in such studies is the absence of insights into the feedback or interacting processes between both aerosols and meteorology on the snow interface, within the Darwinian – Newtonian nexus, as mentioned in (Feingold et al., 2016). Our study merges these two perspectives, where the Darwinian relevance/sensitivity of coupled variables to snow informs Newtonian process-based cryospheric studies. In Fig. 1, we illustrate a schematic that expresses the motivation and the approach behind this study. The Darwinian perspective highlights the individual aerosol and meteorological quantities (along with topography) that couple among themselves and impact snow properties. On the other hand, the Newtonian view encourages a system-wide perspective of the atmosphere-cryosphere interface by exploring the physics-based processes at the interface, namely aerosol deposition, modification of snow properties, snow accumulation, and snowmelt. For both perspectives to meet halfway, we consider individual predictors across aerosols and meteorology that are relevant for snow processes at the snow interface (Darwinian) and highlight important interactions that influence snowmelt (Newtonian).

115 We demonstrate a case study of diagnosing Earth system interactions by expanding on R22 to assess the significance of AMI on snow to SCF variability in the late snowmelt season over LSC regions in HMA across multiple reanalysis frameworks. To characterize AMI on snow, we use a diverse set of geophysical variables spanning both aerosols and meteorology from three major state-of-the-art reanalysis datasets (from ECMWF, NASA, and NCAR) along with satellite observations from MODIS (see Sect. 2.1). We provide a robust estimation of AMI on snow's significance employing two regression-based approaches, a statistical multi-linear regression, and an explainable machine learning (ML) model to infer the non-linear interactions between aerosols and meteorology on snow. Our results show a significant contribution of AMI on snow to SCF variability (at least 20%), with absorbing aerosols and large-scale circulation being the dominant processes within AMI that need emphasis in current reanalysis frameworks. Additionally, we compare the importance of AMI using two different model constructs where we find that the higher importance of AMI in an observational versus that in a model construct suggests 1) its relevance and 2) a lack of adequate representation of AMI-related processes across the reanalyses. We utilize network visualizations and joint distributions to visualize the geophysical quantities interacting within AMI across the reanalyses to demonstrate the degree of coupled parameterizations incorporated in the respective models. Our analysis emphasizes that accurately attributing drivers to any Earth system phenomenon through models depends significantly on how interactions within the Earth system



are represented in coupled ESMs. This accurate representation is crucial for monitoring such Earth system phenomena across
130 climate-vulnerable regions.

2 Methods

2.1 Reanalyses

ERA5 and its land counterpart ERA5-Land are the most recent fifth-generation reanalysis datasets from ECMWF (European
Centre for Medium-Range Weather Forecasts) available from 1979 to the present (Hersbach et al., 2020; Muñoz-Sabater et al.,
135 2021). MERRA-2 is the most recent reanalysis from NASA GMAO (Global Modeling and Assimilation Office) with data
available from 1980 to the present (Gelaro et al., 2017). Both datasets are observationally constrained by assimilating multiple
satellites and in-situ data. It should be noted that snow cover assimilation in ERA5-Land is limited as data above elevation
of 1500 m is not assimilated while most of the study domain lies above this threshold. A relevant difference between the two
reanalysis frameworks is 1) the inclusion of online coupling between aerosol and radiation in MERRA-2, whereas in ECWFM,
140 the radiation scheme uses an aerosol climatology instead; and 2) a separate reanalysis (CAM5-EAC4) for atmospheric com-
position from ECMWF exists, while aerosol products are already simulated within MERRA-2 (Inness et al., 2019; Randles
et al., 2017). We hereafter refer to the ECMWF reanalysis, ERA5 with CAM5-EAC4 as ERA5/CAM5. In addition to these
publicly available reanalyses, we also use a recent, regional reanalysis product from NSF NCAR (National Center for At-
mospheric Research) called MATCHA (Model for Atmospheric Transport and Chemistry in Asia) consisting of 16 years of
145 hydrometeorological and aerosol fields over HMA, generated using the WRF-Chem v3.9.1 (Weather Research and Forecasting
Model with Chemistry) coupled with the CLM-SNICAR model (Community Land Model – Snow Ice Coupled with Aerosol
and Radiation) (Kumar et al., 2024; Flanner et al., 2021; Oleson et al., 2010; Skamarock et al., 2008). The model framework in
MATCHA couples variables between aerosols, meteorology, and land in two ways 1) the Rapid Radiative Transfer Model for
General Circulation Models (RRTMG) allows for online interaction between simulated aerosols and radiation and 2) the use of
150 SNICAR with CLM is an additional component in MATCHA that modifies snow albedo due to deposition of LAPs (Archer-
Nicholls et al., 2016; Mlawer et al., 1997; Kumar et al., 2014). Similar to the reanalyses from ECWFM and NASA, MATCHA
is observationally constrained by daily assimilation of MODIS AOD and MOPITT CO products (acronyms explained in Ap-
pendix B) to constrain the concentration and deposition of LAPs in Asia. These reanalyses encompass different meteorological
models and representations of aerosol processes that make them suitable candidates for understanding the representation of
155 interactions in each model framework. The general characteristics of these datasets are available in Supplementary Table 1.

A total of 22 variables (6 aerosol, and 15 meteorology-related) from the three reanalysis datasets in addition to elevation
were selected as predictors that can potentially drive SCF. The meteorological variables, defined hereafter as MET include a)
temperature (2-m temperature and skin temperature), b) cloud cover (total, low, mid, and high-level cloud cover fraction), c)
dynamic circulation (mean sea level pressure, geopotential height at 500 hPa and 300 hPa, 10-m zonal and meridional winds),
160 d) surface energy fluxes (surface sensible and latent heat), and e) moisture (2-m specific humidity, daily accumulated total
precipitation). The choice of these variables was guided by previous studies showing temperature, precipitation, surface energy



fluxes, and cloud cover are important factors across snow variability studies (Duan and Wu, 2006; Ohmura et al., 1992; Shi et al., 2013; Södergren et al., 2018; Wang et al., 2015; Harder et al., 2017; Shi et al., 2011; Senf et al., 2021; Schlögl et al., 2018). The dynamic circulation variables are chosen considering the association of wind-driven processes and atmospheric teleconnections on SCF (Jiang et al., 2019; You et al., 2020).

Aerosol variables, defined as AER hereafter, consist of aerosol optical depth (AOD) at 550 nm and surface mass mixing ratios. These are grouped by species: a) carbonaceous (hydrophilic and hydrophobic BC and organic matter, b) dust, c) sulphate, and d) others (sea-salt surface mixing ratio including total AOD at 550 nm). Note that MATCHA does not separate carbonaceous aerosols into hydrophobic and hydrophilic components and uses an internal mixing assumption of different aerosol species from emissions. Supplementary Table 2 provides an overview of the variables used in the reanalyses.

In addition to aerosol and meteorological variables, we used elevation (defined as ELEV) from the Global Multi-resolution Terrain Elevation Data (GMTED 2010) as a static predictor to represent topography and its related interactions (Pepin et al., 2015; Danielson and Gesch, 2011). Although snow hydrology is found to be sensitive to not only elevation but also other topographical factors like aspect, slope, and shadowing effects, we use only elevation for this study as a common static predictor to represent topographical interactions across the three reanalyses (Hao et al., 2021).

2.2 Satellite Data

We use MODIS-based Level 3 daily satellite products with a horizontal resolution of 0.05° , namely snow cover fraction (SCF) from MOD10C1/MYD10C1 Collection 6.1, AOD at 550 nm from MODIS processed using the MAIAC algorithm (MCD19A2CMG version 6.1), and land-surface temperature (LST) (MOD11C1/MYD11C1 Collection 6.1) (Hall and Riggs, 2021b, a; Lyapustin, 2023; Wan et al., 2015a, b). We chose to assess our understanding of snowmelt using SCF as 1) it is recognized as an essential climate variable, 2) shown to determine the strength of snow albedo feedback, and 3) shows higher sensitivity to snow albedo feedback than snow albedo in some studies (World Meteorological Organization (WMO), 2022; Qu and Hall, 2007; Fernandes et al., 2009). This choice was also influenced by SCF's broad applicability to various stakeholders for hydroclimate studies in data-sparse regions (Crumley et al., 2020). MODIS LST contains daily data for both day and night, averaged to a daily estimate of LST. MODIS LST is used as a surrogate variable for skin temperature from each reanalysis (Jin and Dickinson, 2010). SCF and LST products from MODIS contain products from both satellites Terra and Aqua, which were averaged to a single quantity for this study. We also use daily accumulated precipitation from IMERG (post-processed final runs) with a spatial resolution of 0.1° to represent precipitation over HMA (Huffman et al., 2014). The acronyms used here are listed in Appendix B.

2.3 Regridding the Data

The finer pixels of the predictors from both reanalysis and satellites were spatially averaged to 0.75° , considering that AER variables from CAMS-EAC4 are available only at 0.75° . Hourly to 3-hourly products from each reanalysis (ERA5/CAMS4, MERRA-2, and MATCHA) were averaged to daily data between the years 2003 and 2018. An exception is the daily accu-

195 mulated precipitation from the three datasets, which was calculated by aggregating (summing) the hourly products into daily products.

2.4 Glacier Regions

A total of 6 glacier regions (GRs) are defined for HMA following the classification in Randolph Glacier Inventory version 6.0 (RGI Consortium, 2017). A total of 15 second-order glacier regions were aggregated into 6 major GRs for this study (Roychoudhury et al., 2022) (see Supplementary Fig. 1). These GRs refer to the geographical extent of the snow-covered regions containing the individual glaciers. The geographical extent of the GRs over HMA is shown in Supplementary Fig. 1a. GRs marked in red (blue) denote regions of high snow cover or HSC (low snow cover or LSC) and have been identified using the methodology described in R22. We specifically focus on the late snowmelt season, i.e., May-July across the years 2003-2018 when AMI is found to be significant in LSC (blue) regions (Roychoudhury et al., 2022). The spatio-temporal mean (standard deviation) across LSC regions during 2003-2018 is 2.4% - 5.5% (5.6% - 9.1%). HMA has an average altitude of 4 km, with a large number of the highest mountains and plateaus in the world across both the LSC and HSC regions. The region is typically arid, with humid summers due to the Asian monsoon. The vegetation type is mostly grasslands and forests with vegetation greening mostly concentrated in LSC regions as well as foothills of HSC regions within the recent decades (Liu et al., 2022, 2021b; Maina et al., 2022).

2.5 Regression Framework to Estimate the Importance of AMI on Snow

210 We regress the target variable (daily SCF) on 22 predictors spanning aerosols (AER), meteorology (MET), and elevation (ELEV) following the equation,

$$Y_{SCF}^{s,t} = \underbrace{\sum_p \alpha_p X_p^{s,t}}_{\text{Term 1}} + \underbrace{\sum_{p,q} \alpha_{pq} X_p^{s,t} X_q^{s,t}}_{\text{Term 2}} + \underbrace{\alpha \mathbb{O}(X^{s,t})}_{\text{Term 3}} \quad (1)$$

where α is the importance/sensitivity of the predictors (X) in regulating SCF (Y), p and q denote sets of different types of predictors (AER, MET, and ELEV) with the superscripts s and t denoting the spatio-temporal dependency of the quantities. Term 1 represents the linear sensitivity of SCF as a function of the AER, MET, and ELEV variables (the predictors X). Terms 2 and 3 introduce non-linear effects that account for interactions between different predictors. Term 2 focuses specifically on product interactions influencing snow grouped as, 1) aerosol-meteorology interactions (AMI); 2) aerosol-elevation interactions (AEI); 3) meteorology interactions (MMI); and 4) elevation-meteorology interactions (MEI) with AMI as the primary focus in this study. In contrast, Term 3 points toward higher-order unresolved processes extending beyond second-order product interactions in Term 2. We select daily products of the target and predictor variables over a 0.75° by 0.75° grid, grouped by 6 glacier regions (GR) and 3 months within the late snowmelt season (May-July).

The importance α is estimated using two distinct metrics: 1) relative importance (RI) from multi-linear regression, and 2) Shapely contribution (SHAPc) from ML (discussed in Sect. 2.6 and 2.7). RI quantifies the importance of Terms 1 and 2 in Eq.



(1), where we only fit the linear (Term 1) and product terms (Term 2) in a multi-linear regression model, while SHAPc is a bulk
 225 measure of the importance of the three terms. While the regression model is an additive combination of individual and product
 terms, the ML model is trained only on the individual predictors. Both metrics are calculated to add up to 100%, making it
 easier to interpret these sensitivities. Note that the metrics of importance are bivariate, reflecting the joint sensitivity of SCF
 to a predictor in the presence of another predictor. Importance of AMI on snow can thus be interpreted as the impact of MET
 predictors on snow in the presence of AER variables.

230 Our notion of importance parallels the chain rule representation (the Darwinian paradigm) of the extensively studied ACI in
 the context of cloud radiative forcing, with cloud fraction/cover as one of the dependencies. While the product of sensitivities
 in the chain rule formulation may not fully capture the non-linear feedback (interaction) between its dependencies, we can
 draw a direct link between the importance of aerosol-cloud cover interactions in our definition of AMI and ACI-cloud cover
 sensitivity from past studies (e.g., Feingold et al., 2016).

235 2.6 Relative Importance Analysis (RIA)

A multi-linear regression (MLR) model was used to regress daily SCF (Y) on a total of 253 predictor variables represented by
 the equation,

$$Y = \sum_{i=1}^{22} \alpha_i X_i + \sum_{i,j=1; j \neq i}^{231} \alpha_{ij} X_i X_j \quad (2)$$

$$= \sum_{i=1}^{22} \left(\alpha_i + \sum_{j \neq i}^{21} \alpha_{ij} X_j \right) X_i \quad (3)$$

240 where $N (= 22)$ is the total number of predictors (see Fig. 1) representing the main effects, in addition to (${}^N C_2 - N = 231$)
 non-linear interaction terms defined as product terms between these predictors (253 in total). We explicitly define second-
 degree interaction terms in the MLR model (only non-square terms) shown in Eq. (2) to represent the non-linear sensitivities
 of our predictors to the SCF variability for each GR and each month in the late snowmelt season. The interaction terms belong
 to five groups, namely: 1) AER-AER 2) AER-MET 3) AER-ELEV, 4) MET-ELEV, and 5) MET-MET. Eq. (3) offers us an
 245 alternate understanding of such an interaction, where the dependence (α) on a predictor X_i is not a constant, but dependent on
 a second predictor (X_j). AMI on snow is defined herein as the sum of α (the importance on modulating SCF) for each predictor
 in the groups AER-AER and AER-MET along with the main predictors from AER. We considered AER-AER to capture the
 snowmelt response to the bulk effect of aerosols in the presence of meteorology.

We estimate the importance (α) of the main and interaction terms using relative importance analysis (RIA) that overcomes
 250 the issue of correlated predictors (very likely in our case) (Tonidandel and LeBreton, 2011). In line with our definition of
 importance, RI quantifies the impact of each predictor (both main and interaction effects) on SCF through fractional contri-
 bution to the total explained variance (R^2). Consequently, RI values sum up to unity or 100% and can be thus expressed as a



percentage. A bootstrapping procedure using subsampling is implemented to generate confidence intervals for the RI estimates (Bickel et al., 2012). Details of the RI implementation are available in Roychoudhury et al. (2022).

255 2.7 Shapley Additive exPlanations using eXtreme Gradient Boosting (SHAP-XGBoost)

We use a robust ML technique called eXtreme Gradient Boosting (XGBoost) that approximates and aggregates predictor-target relationships gradually using subsets of a dataset (Chen and Guestrin, 2016). As in the MLR model, we train XGBoost on the predictors and target for each month (May-July), each GR, and each construct. XGBoost consists of multiple hyperparameters that determine its performance. We use a Bayesian optimization technique called adaptive Tree-Parzen estimators (ATPE) to
260 find the optimal hyperparameters by minimizing the squared error between the true SCF and predicted SCF (Bergstra et al., 2015). The model is trained until we achieve an R^2 (total explained variance) of 95% or more. In contrast to the MLR model (see Sect. 2.6), we do not explicitly define second-order terms for the predictors in the XGBoost model. Instead, we exploit the complex architecture of XGBoost to capture higher-order terms from the 22 main predictors to prevent user-defined bias during the training.

265 The ability of ML algorithms to model non-linear relationships between the target and predictors comes with the cost of decreased interpretability, given the intricate structure of XGBoost needed to model complex target-predictor relationships. The traditional model-dependent approach to interpret interactions in XGBoost models is through estimating feature importance and understanding decision pathways within the models (Jiang et al., 2009). Although various model agnostic interpretability frameworks exist for complex ML models, we interpret our trained XGBoost models using the Shapley Additive explanation
270 (SHAP) framework based on game theory, which quantifies the contribution of predictors and their interactions to the target response (Lundberg et al., 2020). Keeping in line with our definition of importance, we use SHAP to quantify the change in the target due to each predictor (the main effects) and their pairwise interactions. Thus, we can decompose the difference in predicted SCF into 253 ($N + {}^N C_2 - N = 22 + 231 = 253$) individual contributions for each XGBoost model, out of which 22 represent the main predictors and 231 represent the pairwise interaction contribution to the target. Instead of R^2 as in
275 MLR, each SHAP value (for a predictor) represents a fraction of the magnitude of SCF. The SHAP values were normalized to percentages, defined hereafter as SHAPc, by averaging the absolute SHAP values and dividing by their sum. This enables an analogous comparison to the RI metric as a percentage contribution to the total SCF (target) response.

2.8 Leveraging Model Constructs

We perform our analysis based on three model constructs: 1) the Observation-to-Model (Obs-Model) Construct, where SCF
280 from MODIS is the target variable; 2) the Model-to-Model (Model-Model) Construct, where SCF from each reanalysis dataset is the target against corresponding predictors; and 3) the Observation-to-Observations (Obs-Obs) Construct, where we chose a set of variables directly observable through satellites (MODIS SCF, MODIS LST, MAIAC AOD, and IMERG PRECIP) to explore the non-linear sensitivities between SCF and its predictors depicted in Eq. (1).

The utility of these constructs lies in their ability to represent the true Earth system response based on the sensitivity of a
285 target phenomenon, such as snowmelt to its drivers (predictors) and their interactions. The Obs-Obs construct is considered

the closest to ground truth, as it relies solely on observational data but may be overestimated since not all potential drivers are currently observed. The Obs-Model construct also can depict the true response of these interactions but has an inherent bias in the drivers that the models simulate. Conversely, the Model-Model construct captures the sensitivity of the target phenomenon to its predictors as defined by the model design, offering insights into the schemes and parameterizations defined in the model.

290 The regression approach from Eq. (1) is reserved only for the Obs-Model and Model-Model constructs, while the Obs-Obs construct is solely used to elucidate AMI that can be observed through satellites (see Sect. 3.4). This is due to the lack of a diverse range of predictors available from observations with consistent spatio-temporal coverage, a gap that can be bridged by reanalysis products.

Importance estimates in the Obs-Model construct encompass all three terms in Eq. (1) (especially the unresolved stochastic processes driving SCF in Term 3 of Eq. (1) and are the closest approximation to an observable estimate of AMI. The Model-Model construct sheds light on the representation of cryospheric processes driven by AMI in each reanalysis. Comparing the Obs-Model and Model-Model constructs can thus provide insights into the processes in Term 3 of Eq. (1) and highlight any potential misattribution of importance, or underrepresented processes estimated in any of the terms within the Model-Model construct.

300 **3 Results**

The motivation behind this analysis lies in the difference in SCF across satellites and reanalyses. In Supplementary Fig. 1, we show the average spatial distribution of SCF in the late snowmelt season across four data sources (MODIS from satellite, ERA5-Land, MERRA-2, and MATCHA as reanalyses. SCF is very high in ERA-Land which can be attributed to precipitation bias leading to excessive snowfall in the ECMWF snow model, while extremely low SCF in MERRA-2 can be attributed to the high snow depth specified in its land model to consider 100% SCF, leading to lower SCF (Orsolini et al., 2019). This disparity in SCF across different datasets alludes to diverse model representations of processes driving SCF, which we try to leverage in this study. SCF in MATCHA closely resembles that of MODIS, which is a possible result of CLM-SNICAR coupling within MATCHA's model framework, effectively constraining SCF.

3.1 Quantifying Importance of AMI to SCF

310 As mentioned in Sect. 2, we consider 22 different predictors spanning aerosols (AER), meteorology (MET), and elevation (ELEV) from the three reanalyses and regress them on SCF using statistical and machine learning regression methods. We focus specifically on the interacting terms between aerosols and meteorology, defined as aerosol-meteorology interactions on snow (AMI on snow) for our work. Our analysis is based on the importance estimates from the regression algorithms, which denote the sensitivity of the 22 predictors and their higher-order (second-order and/or more) terms to the target variable (SCF). This sensitivity is quantified by two metrics, relative importance (RI) from multi-linear regression (Section 2.6) and Shapely contribution (SHAPc) from ML (Section 2.7). We also use two model constructs on this regression framework to distinguish between the importance of AMI on snow from an observational (Obs-Model construct) and reanalysis (Model-Model construct)



point-of-view. The key point to note is that the target variable (SCF) in the regression is used from two sources: 1) satellite data from MODIS for the Obs-Model construct, and 2) each reanalysis model for the Model-Model construct.

320 In Fig. 2, we show the RI and SHAPc importance distributions of AMI and MMI on snow in the Obs-Model (2b) and Model-Model construct (2c) for LSC regions in the late snowmelt season. The statistics (mean and standard deviation) of the importances for AMI on snow are summarized in Table 1. RI and SHAPc importances for MMI on snow are higher than that for AMI across all datasets with an average contribution of 50-70% (both RI and SHAPc) to SCF variability. AMI on snow shows a consistent magnitude across all datasets in the Obs-Model construct with an average RI of 10-20% and SHAPc of 325 20-35%, indicating a significant contribution to SCF variability. In the Model-Model construct, the mean of the RI and SHAPc distributions for AMI on snow are lower by an average of 10% than in the Obs-Model construct. The spread in the importance distribution of AMI on snow across the constructs and datasets (σ from 1.7 to 7.6 in Table 1) is higher than the difference in the mean importance of AMI on snow for both RI (difference μ difference by 4.5) and SHAPc (difference in μ by 8.2). A non-parametric Mann-Whitney test of the AMI on snow distributions (both RI and SHAPc) shows a significant difference (95% 330 level) for both constructs across the three datasets. AMI on snow is thus significant for both constructs and a lower AMI on snow importance in the Model-Model (relative to Obs-Model) construct suggests second and/or higher-order interaction terms that may be missing or unresolved within the reanalysis model framework (see Sect. 2.5). The large spatio-temporal variability of SCF (Supplementary Fig. 1) in the late snowmelt season, combined with the difference in AMI's importance to snow across both constructs suggests the disparity in AMI-related processes that drive SCF within each reanalysis dataset. SHAPc values 335 for AMI on snow are higher in both constructs compared to RI, which can be due to the ability of XGBoost to capture the non-linear interactions to a fuller extent, compared to the MLR model, where the interactions are restrictive in its definition (only non-square product terms).

3.2 Process Drivers of AMI on Snow

We further decompose the importance of AMI on snow in both the constructs by meteorology (MET variables with five 340 subgroups of variables) and aerosols (AER variables with four subgroups of variables) in Fig. 2a and 2d. Among AER variables, carbonaceous aerosols and total AOD at 550 nm (Others) contribute significantly to the AMI on snow importance (average 18% and 14% respectively) followed by dust (average 11%) in both the constructs and metrics. Among MET variables, circulation-related variables contribute the highest (average 13%) followed by cloud cover variables (average 10%).

An alternate way to visualize the contribution of each subgroup of variables across AER and MET predictors is shown in 345 Fig. 3. We see that circulation variables contribute the most (38%) to AMI on snow in the Obs-Model construct, whereas radiation and temperature dominate (23%) in the Model-Model construct. Carbonaceous variables are dominant across both constructs (30%); however, dust contributes more in the Obs-Model construct (24%) than in the Model-Model construct (20%). Additionally, the AER subgroup Others (including total AOD at 550 nm and surface sea-salt) makes a significant contribution, primarily driven by total AOD at 550 nm.

350 The prevalence of carbonaceous aerosols can be attributed to increased surface BC and total aerosol optical depth (AOD) in the vicinity of the LSC regions during the pre-monsoon season (April-May). This includes wheat crop residue burning in



the northern part of the Indian subcontinent inducing potential interactions with large-scale synoptic atmospheric circulation in the subsequent months (late snowmelt season) that lead to changes in near-surface temperatures, convection, and accelerated melting (Das et al., 2022; Kumar et al., 2011; Lau et al., 2006; Ramanathan et al., 2007; Lau and Kim, 2018). Such interactions can also allude to the deposition of LAPs through interactions between aerosols, geopotential height, and near-surface variables. Multi-model intercomparison of global aerosols has also reported that carbonaceous aerosols contribute an average of 70% to aerosol-induced absorption, a key process in AMI on snow (Sand et al., 2021). A higher importance can be seen across the predictor subgroups and datasets in AMI on snow distributions within the Obs-Model relative to the Model-Model construct for both metrics. This can be attributed to the absence of unresolved processes and their interactions driving SCF in the model representation of the three reanalyses. It can however be the case that the observations are biased or that the modeled SCF might not be spatially or temporally in phase with MODIS SCF. With the current observing system, we cannot attribute this difference in importance to the errors in the observations, the models, or a combination of them.

The metrics, RI, and SHAPc highlight two aspects of these interactions. The SHAPc distribution of AMI's importance onto snow has a higher spread (σ between 5.6 - 7.6) indicative of a bulk non-linear effect. This is seen in Eq. (1) where SHAPc reflects the sensitivities in all three terms. Whereas for RI, the lower spread in the distribution of AMI's importance on snow (σ between 1.7 to 3.2) indicates specific (local) second-order processes captured by RI (first and second term in Eq. (1)).

3.3 Emergent Connections within AMI

Moving beyond the types of AER and MET predictors that dominate AMI on snow, we show in Fig. 4 the importance of individual interactions within AMI across both model constructs, both importance metrics, and three reanalysis datasets, using concepts from network analysis (Inglis et al., 2022). For each of the twelve networks, the six larger nodes (circles) represent the AER predictors while the smaller nodes represent the MET predictors. The connections (edges) between them are weighted by the pairwise importance according to the importance metric (RI and SHAPc) to represent the interactions (edge connections) and their strengths (edge widths and colors) between AER and MET variables on the snow interface. The node sizes depend on the degree of each node (number of edge connections per node weighted by the edges). For a total of 21 predictors, these would lead to $\frac{21C_2}{2} = 105$ edges across 21 nodes for each network. These edges are weighted by their color and width according to their interaction importance (between 1 to 100%). Since we are considering interactions related to AMI on snow, we consider the pairwise interactions of 6 AER predictors with 15 MET predictors. As such, the degree of the AER nodes will be much higher than those of the MET nodes. The weighted degree is defined in Appendix A. This can be seen from the networks in Fig. 4 where the AER nodes have a larger size relative to the MET nodes. In the following sections, we primarily focus on the weighted edges of these networks as the degrees of the AER nodes are relatively similar across the networks.

3.3.1 Observed versus Model Snow Interface

A prominent feature across all the networks is the difference between the interactions seen between the two constructs across the three reanalyses. The networks in the Obs-Model Construct show a higher number of *strong* (> 50% importance, moderate to very high) interactions whereas the networks in the Model-Model construct show fewer and specific *strong* interactions.



385 This suggests greater interaction strength/importance between the AER and MET predictors that contribute to the target (SCF) variability compared to what the models in each reanalysis show. The higher density of connections within the Obs-Model construct suggests significant AMI-related interactions at the *real snow interface*, compared to what the models in the reanalyses consider to be relevant for the *model snow interface*. This agrees with our observations from Fig. 2 and Table 1 where the distribution of AMI's importance on snow in the Obs-Model construct is statistically significant compared to that in the
390 Model-Model construct. Additionally, as discussed in Sect. 2.8, the interactions shown in the Obs-Model construct can reflect physical reality while the Model-Model construct only captures the interactions that the model frameworks parameterize within themselves. In Table 2, we present the dissortativity of the networks depicted in Fig. 4 (Newman, 2002) (defined in Appendix A). Dissortativity measures the diversity of interactions between the AER nodes and the MET nodes. Our results show that dissortativity is highest for the Obs-Model construct compared to the Model-Model construct, indicating greater diversity in
395 AMI on snow interactions within the Obs-Model construct.

To highlight the difference between the two constructs, Fig. 5 shows the aggregated (summed) interactions between AER and MET variables for each construct and importance metric across all three reanalyses. This demonstrates the interactions that each construct generally emphasizes. We also show the positive difference in the interactions between the Obs-Model and the Model-Model construct (in Fig. 5c) for each metric, which can highlight specific interactions missing in the modeled
400 reality (Model-Model construct). Both RI and SHAPc emphasize interactions of surface dust (DU) with circulation variables (particularly geopotential height at 300 hPa and 500 hPa as well as mean sea level pressure) in the Obs-Model construct, which are weaker in the Model-Model construct. We see this in Fig. 5c, where both difference networks for both metrics highlight strong interactions with the circulation variables, suggesting that interactions of circulation variables, particularly with dust is missing in the Model-Model construct. RI also shows missing interactions with temperature variables in the difference network,
405 which is not visible for SHAPc. On the other hand, SHAPc emphasizes moderate-high (50% to 75%) interactions with cloud cover variables (particularly medium, high, and total cloud cover) that are missing in the Model-Model construct.

3.3.2 Varying Orders of Interactions

Comparing the networks between the RI and SHAPc metrics provides insights into how each of these two metrics highlight the functional aspect of AMI on snow. As mentioned in Sect. 2.5, RI, and SHAPc highlight different orders of interactions
410 based on their definitions. In Fig. 4, we can see that RI importance metric focuses more on specific interactions while the networks for the SHAPc metric appear more interconnected, with a broader distribution of importance values. In Fig. 5, we see that interactions of surface dust (DU) are the strongest across both metrics, but RI emphasizes product interactions with temperature and surface energy variables (particularly surface sensible heat flux or sShf), while SHAPc captures the higher-order interactions with temperature across both constructs. Both metrics fail to capture interactions with circulation, which
415 can be seen in the difference networks in Fig. 5c. This emphasizes the need to include circulation-related interactions in the model frameworks of all three reanalyses. From the difference networks, we can visualize how SHAPc and RI metrics differ between the constructs and highlight higher-order processes that are inadequately represented in the model framework of each reanalysis. We see that *strong* second-order interactions (from RI) of DU and AOD550 with temperature and circulation



variables are underrepresented in all three reanalyses, while *strong* higher-order interactions of AER variables with cloud cover
420 and circulation are missing across all the reanalyses. However, SHAPc does capture temperature interactions in both constructs.
Higher dissortativity in the three reanalyses (Table 2) for the SHAPc metrics in the Obs-Model construct suggests a greater
variety of higher-order processes across AER and MET predictors at the *observed* snow interface compared to the *model* snow
interface.

3.3.3 Coupling Strength across the Reanalyses

425 From Supplementary Fig. 1, SCF from MATCHA agrees most with the observed SCF during the study period (May to
July). This can be attributed to the stronger coupling within MATCHA's model framework, which couples aerosols, radiation,
and snow, in comparison with the other two reanalyses. This is also reflected in the density of the connections observed
in MATCHA, particularly in the Obs-Model construct from Fig. 4a, relative to that of ERA5/CAMS4 and MERRA2. Despite
the tighter coupling in MATCHA, there are notable differences between the networks across the constructs. In the individual
430 networks in Fig. 4, the Model-Model construct for MATCHA emphasizes interactions with carbonaceous aerosols, whereas
the Obs-Model construct highlights dust (DU). Ideally, the interactions in the Model-Model construct should be similar to
that in the Obs-Model construct. However, significant differences between the constructs across all the reanalyses can indicate
interactions that are inadequately represented in each reanalysis. We explore these differences further in Fig. 6, where we show
the underrepresented interactions across all the reanalyses (using the positive differences between the importance seen in the
435 Obs-Model and the Model-Model construct aggregated across RI and SHAPc). For MATCHA, the major deficiency lies in representing
interactions of DU and carbonaceous aerosols with circulation variables (particularly geopotential height and mean
sea level pressure). Further analysis of these interactions (as shown in Supplementary Fig. 2) reveals that MATCHA fails to
adequately represent the second-order interactions (based on RI) of DU with circulation, temperature, and surface energy variables,
as well as the higher-order processes (based on SHAPc) involving absorbing aerosols with circulation and cloud cover
440 variables. We show the underrepresented interactions (positive difference between Obs-Model and Model-Model construct)
for different orders across each reanalysis, based on RI and SHAPc in Supplementary Fig. 2.

While MATCHA exhibits denser connections in the Model-Model construct compared to ERA5 (Fig. 4), the density of the
interactions for MERRA2 is closely comparable to that of MATCHA, despite differences in individual interactions. This is
further evident in Fig. 6 where the underrepresented interactions in MATCHA and MERRA-2 are significantly less compared
445 to ERA5/CAMS4, indicating stronger coupling in both models. Both MERRA-2 and ERA5/CAMS4 show insufficient interactions
with circulation and temperature variables. However, ERA5/CAMS4 exhibits a greater deficiency in these interactions,
extending to cloud cover as well. Detailed analysis of the missing interactions based on their order (across RI and SHAPc from
Supplementary Fig. 2) reveals that in MERRA-2, second-order interactions between DU and AOD with circulation and temperature
variables are absent, as well as higher-order processes between dust and geopotential height. In ERA5/CAMS4, the
450 density of the underrepresented interactions in Fig. 5 shows that a large number of interactions are not represented adequately
in its model framework, with significant gaps in second and high-order processes involving cloud cover. Dissortativity values
from Table 2 show that while all three reanalyses show higher diversity of AMI on snow in the Obs-Model construct, both



MERRA-2 and MATCHA have the highest dissortativity in the Obs-Model construct, especially for higher-order processes (represented BY SHAPc).

455 Another approach to understanding the inadequate processes in the reanalyses is to compare the interactions of ERA5/CAMS4 and MERRA-2 across the two constructs with that of MATCHA. Given the strongly coupled nature of MATCHA, Supplementary Fig. 3 specifically highlights predictor interactions that ERA5/CAMS4 and MERRA-2 fail to capture compared to MATCHA. The interactions are estimated as before by taking the positive difference between the importance of ERA5/CAMS4 and MERRA with MATCHA for each construct. Both constructs demonstrate a lack of interactions with circulation variables
460 in the two reanalyses, shown by the presence (absence) of strong edge connections between circulation and AER variables in the Obs-Model (Model-Model construct). Additionally, meteorological interactions with DU are more pronounced in the Obs-Model construct, in contrast to their almost minimal contribution in the Model-Model construct, where carbonaceous aerosols are more significant. The networks indicate that significant interactions of aerosols with circulation variables should be present in both reanalyses, although MATCHA also fails to adequately capture the circulation interactions as seen in Fig.
465 6. Specifically, ERA5/CAMS4 should focus more on circulation interactions with DU, while MERRA-2 should emphasize interactions with carbonaceous aerosols to capture the coupling within MATCHA.

3.3.4 Potential Misattributions in each Reanalysis

In addition to highlighting the underrepresented interactions through the difference networks, we hint towards potential misattributions in each reanalysis through Fig. 6 by examining interactions that are strong in the Model-Model construct but absent
470 in the Obs-Model construct. This is estimated using the negative difference of importances between the Obs-Model and the Model-Model construct (shown through red edges) instead of the positive difference for the underrepresented interactions (through black edges). These discrepancies highlight significant interactions and processes that the models consider important for the *model* snow surface but cannot capture for the *observed* snow surface. Specifically, we find that MERRA-2 and MATCHA overemphasize the interactions between dust (DU) and accumulated precipitation (PRECIP), while ERA5/CAMS4
475 places undue importance on the interactions between dust (DU) and skin temperature (SKT), even though interactions with 2-m temperature is much more significant in the Obs-Model construct. Although these interactions are related to temperature, the disparity here suggests that feedbacks between surface dust aerosols and near-surface temperature are more significant than those involving the surface itself.

An associated issue with misattribution is the buffering of the snowmelt response from one predictor due to the presence of
480 other predictors which can obscure the true influence of especially the aerosol predictors on snowmelt, resulting in inaccurate conclusions about their relative contributions. Buffering of the interaction sensitivity by other dominant predictors is seen in aerosol-cloud-precipitation interactions, where different cloud processes can buffer the sensitivity of aerosols to precipitation (Stevens and Feingold, 2009; Michibata et al., 2020). Although we can potentially highlight where each model misattributes the snowmelt sensitivity for AMI interaction, we are unable to determine the buffering of snowmelt response of AER predictors
485 by the MET variables with the current approach.



3.3.5 Bringing it altogether

The networks reflect the complexity of each reanalysis, and their ability to capture the feedbacks between the AER and MET variables for both observable and modeled realities (the constructs). The progression in importance, in terms of both the number and strength of interactions from ERA5/CAMS4 to MATCHA (both number and strength of interactions) from ERA5/CAMS4 to MERRA-2 TO MATCHA across both constructs signifies the degree of coupling incorporated in the three reanalyses, This
490 progression reflects the absence of coupling between aerosols and meteorology in ERA5/CAMS4, in contrast to MERRA-2 and MATCHA.

The degree, or the number of relatively stronger connections to a node (each predictor), reflects the magnitude of the coupling processes in ESMs, both direct and indirect. However, the edge strength is a function of the abundance (magnitude) and
495 co-variability of the interacting predictors (nodes) and indicates the importance of the coupling/interaction. Visualizing the number and strength of each interaction within AMI on snow through the network diagrams highlights relevant processes of different orders driving SCF during the study period. These interactions are otherwise difficult to disentangle due to their inherent complexity. Using constructs and different metrics of importance allows us to demonstrate which interactions and their complexities are necessary to be represented in each reanalysis model. Additionally, comparing these networks helps identify
500 the misattribution of interacting processes in each reanalysis. This can be analyzed from the interactions present in the Model-Model construct but absent in the Obs-Model construct. We see that interactions between DU and PRECIP in MERRA-2 and MATCHA are given unnecessary importance, while for ERA5/CAMS4, it is the interactions between DU and SKT that are overemphasized. Overall, the need to incorporate large-scale circulation-related interactions is emphasized across the reanalyses to correctly observe SCF during the study period. Uncertainties associated with atmospheric circulation is a pertinent
505 problem across climate models due to internal variability of the Earth's climate and errors in model representation (Shepherd, 2014). Interactions of the large-scale circulation dynamics with unresolved small-scale processes involving clouds, convection, the boundary layer, complex topography, and near-surface temperature, remain uncertain across models (Stevens and Bony, 2013; Bony et al., 2015; Holtslag et al., 2013; Sandu et al., 2019). Considering aerosols adds to this uncertainty due to interactions with cloud microphysics, precipitation, and convection, making accurate representation even more challenging (Bony
510 et al., 2015; Dagan et al., 2023; Fan et al., 2012; Mülmenstädt and Wilcox, 2021). Anthropogenic forcings due to greenhouse gases and aerosols cannot be neglected as they have been shown to influence trends in circulation variables like geopotential height at 500 hPa and mean sea level pressure (Christidis and Stott, 2015; Gillett et al., 2013; Ming and Ramaswamy, 2011). Improving the circulation-related interactions with aerosols in coupled ESMs can improve the representation of monsoon, regional and local aerosol transport pathways, aerosol deposition, and cloud distribution in complex regions like HMA (Li et al.,
515 2016; Hu et al., 2024; Mülmenstädt and Wilcox, 2021).

Both BC and dust impact snow by modifying the snow albedo feedback, although their relative importance to radiative forcing remains uncertain. We see in Sect. 3.2 that while BC (as a component of carbonaceous aerosols) dominates the bulk contribution to AMI on snow, individual interactions of meteorology variables with DU become more prevalent when we analyze the networks after decomposing this bulk contribution to AMI. This is also seen across the networks, where the node



520 sizes for BC and DU (based on their weighted degree) are similar, thus alluding to the similar number of interactions with the
meteorology variables. We allude to this disparity in Supplementary Fig. 4 where we see a higher abundance of DU (which has
both natural and anthropogenic sources) than BC (mostly anthropogenic sources) over HMA. The spatial distribution shows
that higher values of surface BC are primarily concentrated in the vicinity of the glacier regions indicating pollution sources
from nearby Asian countries. A higher concentration of surface DU is concentrated in northern HMA especially in the LSC
525 regions due to its proximity to the Gobi and Taklamakan deserts. The monthly variations of BC and DU also show a greater
abundance of DU compared to BC during the study period. The prevalence of inadequate representation of dust and circulation-
related interactions can thus indicate biases in the model to simulate the abundance of these quantities over the LSC regions in
HMA, compared to the biases in simulating BC abundance.

3.4 Observable AMI on Snow

530 Given the significance of AMI in regulating SCF during the study period, it would be useful to interpret what these interactions
within AMI on snow represent through observed relationships between the predictors and SCF. While having multiple pre-
dictors from satellite observations would be ideal for exploring AMI on snow (or any Earth system interactions) to its fullest
extent, we consider four such variables from satellite observations, MAIAC AOD, MODIS LST, and IMERG PRECIP, and vi-
sualize their relationship with MODIS SCF, which we defined as the Obs-Obs construct in Sect. 2.8. Exploring the relationship
535 between predictors in the Obs-Obs construct will provide a basis of ground truth for relative comparison with findings in the
other two constructs, and aid in understanding the relationships between the chosen predictors and their SCF response.

In Fig. 7, we show the relationship between MODIS SCF and the predictors MODIS LST and IMERG PRECIP weighted by
the distribution of MAIAC AOD for LSC regions during May-July. We observe an overall trend of exponential decay of MODIS
SCF with MODIS LST above 0°C, dominated by high values of MAIAC AOD, especially at higher LST and lower SCF. Such
540 behavior can point to the radiative effects of absorbing aerosols causing warmer temperatures (high LST) and accelerated
snowmelt (low SCF). However, this does not imply causality as it might be attributed to the warmest areas in the domain (with
high LST) located at lower elevations and directly affected by air pollution (high AOD), or that spatial resolution of 0.75o
in the datasets might include non-snow-covered regions with high temperatures. We use a mutual information-based metric to
quantify the bulk non-linear association of SCF to LST (as shown by the bars in Fig. 7) (Kraskov et al., 2004). The strongest
545 association between MODIS LST and SCF occurs for low to moderate values of AOD (values within 0.04 – 0.10). Compared
to satellite observations, MATCHA shows a similar relationship between SCF and LST compared to the other two datasets
(for both Obs-Model and Model-Model constructs). Given that MATCHA is the only framework among the three datasets with
coupling between snow, radiation, and LAPs, this similarity confirms the ability of parameterizations in MATCHA to represent
AMI on snow better than datasets from MERRA-2 or ERA5/CAMS4. In the Model-Model construct, MERRA-2 shows the
550 strongest relationship between SCF and LST at moderate to very high values of AOD (0.1 – 6.8) suggesting an overestimated
aerosol loading (compared to AOD in Obs-Obs) in LSC regions during the late snowmelt season that might contribute to the
lower SCF values over HMA seen in Supplementary Fig. 1 for MERRA-2. On the other hand, ERA5/CAMS4 has stronger
SCF-LST sensitivities for values below high AOD (< 0.21), which can allude to a lack of coupling related to aerosol radiative



555 feedbacks within the ERA5 model that translates to an absence of strong SCF-LST dependencies to the AOD distribution in
CAMS-EAC4. The strong SCF response to LST for ERA5 at lower AOD values (below high AOD, <0.21) can either allude
to the buffering of aerosol effect reflected in the lack of coupling within ERA5 related to aerosol radiative feedbacks. This can
thus indicate misattribution of the SCF response to aerosols in the presence of meteorology.

We also see an exponential decay between MODIS SCF and IMERG PRECIP in the Obs-Obs construct, with strong SCF-
PRECIP dependency at low to moderate values of AOD (0.04 – 0.10). This might indicate potential removal (wet scavenging)
560 of absorbing aerosols by precipitation that can result in lesser amounts of exposed absorbing aerosols onto snow, hence re-
ducing snow darkening and its impact on snowmelt (Gryspeerd et al., 2015). As mentioned earlier regarding the SCF-LST
relationship, direct causality is not implied as the wetter areas in the domain (high PRECIP) can be located at lower elevations
and directly impacted by air pollution (high AOD), or that the spatial resolution of 0.75° might include areas with non-snow-
covered regions with high precipitation. MATCHA also exhibits the most similarity in the SCF-PRECIP relationship to the
565 Obs-Obs construct compared to the other two datasets, with strong sensitivity of SCF to PRECIP in the low-moderate AOD
range. This reflects the degree of coupling within MATCHA compared to MERRA-2 and ERA5/CAMS4. MERRA-2 reflects
the underestimation of SCF as seen in Supplementary Fig. 1 and the SCF-PRECIP relationship is strong for moderate to very
high values of AOD (0.1 – 6.8) compared to the other datasets (where the SCF-PRECIP is strong for values below high AOD),
suggesting overestimated AOD within the model (compared to AOD in Obs-Obs) in LSC regions during the study period. High
570 SCF in ERA5/CAMS4 is dominated by low to moderate AOD (0.04-0.10) in the Model-Model construct (as compared to high
SCF when AOD is low or < 0.04 for Obs-Obs). This can indicate higher-than-usual aerosol loading within CAMS-EAC4 in
the study region during the late snowmelt season.

4 Summary and Implications

4.1 Main findings

575 Through our analysis, we diagnosed three reanalysis frameworks in their ability to capture a particular case of Earth-system
interactions, those pertaining to feedbacks between aerosols and meteorology that affect snowmelt over HMA. By employing
a data-driven approach across twenty-two distinct geophysical quantities, we defined aerosol-meteorology interactions at the
snow interface (AMI on snow) over low snow-covered regions (LSC) of HMA through interactions of various orders across
six aerosol and fifteen meteorology variables. Our main findings are as follows,

580 – **Importance of AMI to SCF Variability.** We substantiated the importance of AMI on snow in driving SCF variability
across three reanalyses during the late snowmelt season, building on previous work (Roychoudhury et al., 2022). While
interactions within meteorology at the snow interface (MMI) remain the primary driver of SCF (60% contribution),
drivers related to AMI account for an average 20% of the SCF variability. The robustness of AMI on snow importance
was established by using two regression-based algorithms—one statistical and one machine learning-based—to quantify
585 the importance of non-linear interactions to snowmelt and characterize them within AMI.



- **Significant Drivers within AMI on snow.** By introducing the concept of constructs for the regression algorithms that correspond to observed and model reality (within each reanalyses), we determined which group of aerosols and meteorology variables contribute to most of the importance of AMI on snow. Dominant contributions from carbonaceous aerosols (30%), dust (24%), and large-scale circulation variables (38%) contribute to AMI at the *observed* snow interface, whereas variables related to near-surface temperature (22 %) and surface energy fluxes (23%) are given priority at the *model* snow interface.
590
- **Underestimation of AMI on snow across the reanalyses.** Comparative analysis between the constructs through network visualizations reveals 1) individual interactions between aerosols and meteorology variables that are underrepresented in each reanalysis and 2) the underestimation of AMI's importance to SCF within the reanalyses compared to satellite-based SCF, which highlights a significant disparity between observed and modeled data. Furthermore, by applying the concept of assortative mixing in networks (Newman, 2002), we can observe differences in the diversity of AMI interactions across both constructs for each reanalysis.
595
- **Underrepresented interactions within AMI on snow.** Circulation-related interactions with dust aerosols, particularly those involving geopotential height and mean sea level pressure, are significant yet insufficiently represented in the models within each reanalysis. The importance of circulation-related interactions suggests that extra attention needs to be paid to interactions of aerosols and smaller sub-grid processes with large-scale atmospheric circulation involving clouds, convection, and transport across the boundary layer (Shepherd, 2014; Hu et al., 2024).
600
- **Complexity of coupling across each reanalysis.** Reanalysis from NSF NCAR (MATCHA) strongly resembles the relationships between aerosols and meteorology to observed SCF, considering that the degree of coupling parameterizations interfacing the atmosphere and land (cryosphere) is highest in MATCHA due to the inclusion of feedbacks in its model between aerosol, radiation, and snow through CLM-SNICAR. Using available aerosol and meteorology observations from satellites also shows that MATCHA captures the joint sensitivities between aerosol and meteorology variables observed across satellites. Although both MERRA-2 and MATCHA incorporate some degree of coupling within their models, interactions of dust with circulation variables need more attention within the two. The models in both these reanalyses overemphasize interactions of aerosols (particularly dust) with daily accumulation precipitation, instead of coupling with circulation variables like geopotential height and mean sea level pressure. ERA5/CAMS4 relies extensively on its non-coupled model framework and assimilation of observations and needs extra attention to circulation and cloud cover-related interactions in the future development of the ECMWF model. The variability in the importance distribution of AMI on snow across the reanalyses is also lower than the difference in the variability of AMI's importance on snow from both constructs (Fig. 2 and Table 1) indicating that the coupling within MATCHA is far from ideal. Thus, the need for parameterizations that represent the feedbacks between snow and aerosol abundances, including relevant snowmelt drivers like circulation-related variables is necessary to consider in the development of future ESMs.
605
610
615



– **Physics-informed insights.** The consistent importance of aerosol-meteorology interactions on snow over HMA across two regression algorithms and constructs suggests that the sensitivities observed of these interactions to snowmelt are not merely statistically inferred, but rooted in physics-informed insights. Available observations from satellites confirm these insights by demonstrating similar relationships between aerosol and meteorology variables especially the strongly coupled reanalysis (MATCHA) as seen in Section 3.4. The radiative effect of absorbing aerosols, as well as wet scavenging of these aerosols by accumulated precipitation is seen across the observations and the reanalyses, in addition to their inherent biases in representing these processes.

620

625 4.2 Implications to Earth System Predictability

The synergistic approach across 1) constructs using statistical regression and machine learning methods, and 2) network analysis, proves to be a viable and more economical alternative to expensive feedback separation methods conventional in the community. This highlights the potential in our methodology to detect non-linear relationships not only within the atmosphere-cryosphere interface but also in other Earth system processes. In addition to quantifying the relevance of these coupled processes, this methodology allows us to identify key variables driving these interactions and pinpoint deficiencies in their representation across different models. While current benchmarking frameworks that evaluate Earth system models (ESMs) utilize a diverse range of statistical metrics and their ability to represent diverse climate modes of variability, the approach proposed here can assist in identifying specific interactions that are highly uncertain and complex for any Earth system phenomena, extending beyond snowmelt in the Third Pole (Lee et al., 2024; Lauer et al., 2020).

630

Our results emphasize the necessity to 1) incorporate relevant non-linear interactions pertaining to circulation, temperature, and cloud cover between aerosol and meteorological variables within ESMs in the prediction of snow hydrology, 2) inform specific variables that need to be assimilated in the design of observing systems, and 3) include more observable variables across different Earth system components (such as aerosols and meteorology in this study) in future phases of the Coupled Model Intercomparison Project (CMIP) and its allied ESM-SnowMIP across both aerosols and meteorology to assess their co-variability (Krinner et al., 2018). From our findings in Figs. 2-3 and the individual interactions within the networks in Figs. 4-6, we emphasize the incorporation of variables related to large-scale atmospheric circulation, near-surface temperatures, as well as improved proxies of absorbing aerosols, particularly dust within the future CMIP and ESM outputs. Considering the future direction of ESMs toward Integrated Earth System Model and Analysis (IESM, IESA) with an emphasis on observationally constrained coupled chemistry meteorological models (CCMMs), joint assimilation of AMI-relevant variables is essential for this development (Bocquet et al., 2015; National Academies Press, 2018). Furthermore, with recent pioneering work in training ML forecast models such as GraphCast on ERA5 data (Lam et al., 2023), it is more important than ever to assess the representation of coupling of relevant interactions in existing reanalyses. Diagnosing and quantifying the strength of these interactions across different Earth system processes is critical in reducing uncertainties in Earth system prediction and minimizing the false attribution of observed environmental changes (National Academies of Sciences, Engineering, and Medicine, 2022; Ripple et al., 2023). Identifying the underrepresented interactions in ESMs has the potential to improve medium-range

645

650

and sub-seasonal to seasonal forecasts of high-impact weather, particularly water cycle extremes that can help increase the resilience of vulnerable populations in regions such as HMA (NOAA Science Advisory Board, 2021).

4.3 Limitations and Future Directions

It is important to recognize that while this study specifically analyzes the coupling across aerosols, meteorology, and snowmelt
655 over HMA, our primary motive is to showcase an alternative approach to unravel potentially any Earth system interaction, identify its key drivers, and inform inconsistencies across different models in their ability to represent coupled Earth system processes. While our analysis focuses on low snow-covered regions in HMA and the late snowmelt season, further assessments of AMI in high snow-covered (HSC) regions within HMA and during the snow accumulation period are also necessary. The more transient changes in seasonal snowpacks within LSC regions show significant sensitivity of AMI to snow, while the
660 non-seasonal snowpacks in HSC regions are influenced by longer timescales (Liu et al., 2021a). Preliminary results for HSC regions in Supplementary Fig. 5 also show the strong importance of AMI on snow for these regions, although they have a higher variability (in the spread of the AMI distribution) compared to LSC regions. Additional observational datasets for SCF and other snow properties (e.g., snow albedo) need to be explored to improve the robustness of our findings (Wu et al., 2021; Liu and Margulis, 2021; Rittger et al., 2021). Additional observational datasets across the predictors also need to be explored to improve
665 the robustness of our findings and study the process-level physics between the drivers of these interactions as in Sect. 3.4. While we focus on aerosol-meteorology interactions at the snow interface over HMA, a similar analysis for interactions within meteorology and with elevation will also provide additional insights into the complex processes and their model representation over the Third Pole. We understand that insights from our approach are dependent on the choice of variables to represent these processes, thus future studies incorporating other relevant variables will also prove useful. An additional avenue to venture into
670 would be to separate the misattribution and buffering of the drivers in the identified couplings, which is limited in our current approach. It is also important to note that estimates from interpretability frameworks within explainable ML are dependent on the prediction of the ML model. Thus, a combination of other interpretability techniques and more complex ML algorithms (e.g., deep neural networks) can also add to a thorough understanding of Earth system interactions.

Data availability. Satellite and reanalysis data are available in the public domain. ERA5/ERA5-Land data were downloaded from the Copernicus Climate Data Store available at <https://cds.climate.copernicus.eu/cdsapp#!/search?type=dataset&text=ERA5>. CAMS-EAC4 data were downloaded from the Atmospheric Data Store available at <https://ads.atmosphere.copernicus.eu/cdsapp#!/dataset/cams-global-reanalysis-eac4?tab=overview>. MERRA-2 and IMERG Final Run data were downloaded from NASA GES DISC available at <https://disc.gsfc.nasa.gov/>. MODIS SCF and LST and MAIAC AOD were downloaded from NASA Earthdata <https://search.earthdata.nasa.gov/search>. The MATCHA dataset is recently released at the NSIDC (National Snow and Ice Data Center) for public use at https://nsidc.org/data/hma2_matcha/versions/
680 1. An introductory article on MATCHA's model design is provided at <https://himat.org/topic/matcha/>. The codes for MATCHA's model framework, the regression algorithms, and the analysis will be made available in a public repository after publication.



Appendix A: Measures of Network Properties

A1 Weighted Degree

For a network with N nodes, the weighted degree d_i of node i can be mathematically represented as:

$$685 \quad d_i = \sum_{j=1}^N w_{ij} \quad (A1)$$

where w_{ij} is the interaction importance of the edge between node i and node j .

A2 Assortativity/Dissortativity

Assortativity (dissortativity) in a network measures the tendency of nodes to connect to other nodes with similar (dissimilar) edge weights (i.e. the interaction importance) and lie between -1 and 1. Positive values indicate assortative mixing, which means
690 higher-degree nodes tend to connect with other-higher degree nodes, or in other words, nodes with stronger interactions tend to connect together. Negative values indicate the tendency of higher-degree nodes to connect to lower-degree nodes, or nodes with stronger interactions tend to connect nodes with weaker interactions. For our networks in Fig. 4, we see high negative assortativity (high dissortativity) shown in Table 2. This is because we are measuring the interaction importance of AMI on snow(or aerosol-meteorology interactions on snow) where six of the AER nodes will have a higher degree as they connect
695 with 15 different MET nodes. This leads to dissortativity across all the networks as seen in Table 2. Higher dissortativity for a network indicates that the nodes tends to connect with highly variable interaction importances. This can thus indicate a measure of the diversity of the interactions (here between AER-MET nodes which is AMI) within any given network, where the nodes with higher degrees (AER) are connected across various lower degree nodes (MET). It is quantified by the assortativity coefficient r given by,

$$700 \quad r = \frac{\sum_{jk} jk(e_{jk} - q_j q_k)}{\sigma_q^2} \quad (A2)$$

where e_{jk} is the joint probability distribution of the node degrees, q_j and q_k are the remaining degree distributions, and σ_q is the standard deviation of the distribution q . The joint probability distribution of the node degrees e_{jk} is the probability that an edge connects nodes of degree j and k , where the weighted degree is calculated is using Eq. (A1). Specific details on calculating network assortativity/dissortativity can be found in Newman (2002).

705 Appendix B: Acronyms

ACI Aerosol-cloud interactions

AER Aerosol variables



- AMI** Aerosol-Meteorology interactions at the snow interface
- AOD** Aerosol optical depth at 550 nm
- 710 **ATPE** Adaptive Tree-Parzen estimators
- BC** black carbon
- BrC** brown carbon
- CCMM** Coupled chemistry meteorological model
- CLM-SNICAR** Community Land Model – Snow Ice Coupled with Aerosol and Radiation
- 715 **CMIP** Coupled Model Intercomparison Project
- DU** surface dust mixing ratio
- ECMWF** European Centre for Medium-Range Weather Forecasts
- ELEV** Elevation
- ES** Earth system
- 720 **ESP** Earth system predictability
- ESM** Earth system model
- GMTED** Global Multi-resolution Terrain Elevation Data
- GR** Glacial Regions
- HMA** High Mountain Asia
- 725 **HSC** High snow covered regions in High Mountain Asia
- IESM/IESA** Integrated Earth System Model/Analysis
- IMERG** Integrated Multi-satellite Retrievals for GPM
- LAPs** light-absorbing particles
- LSC** Low snow covered regions in High Mountain Asia
- 730 **MAIAC** Multi-Angle Implementation of Atmospheric Correction
- MATCHA** Model for Atmospheric Transport and Chemistry in Asia



- MET** Meteorology variables
- ML** Machine learning
- MLR** Multi-linear regression
- 735 **MODIS** Moderate Resolution Imaging Spectroradiometer
- MOPITT** Measurements of Pollution in the Troposphere
- NASA GMAO** NASA Global Modeling and Assimilation Office
- NCAR** National Center for Atmospheric Research
- PRECIP** accumulated precipitation
- 740 **RI** Relative importance
- RRTMG** Rapid Radiative Transfer Model for General Circulation Models
- SCF** Snow cover fraction
- SHAP** Shapley additive explanation
- SHAPc** Shapley contribution
- 745 **WRF-Chem** Weather Research and Forecasting Model with Chemistry
- XGBoost** eXtreme Gradient Boosting



Author contributions. CR contributed to the conceptualization, methodology, formal analysis, investigation, visualization, writing-original draft, reviewing, and editing. CH contributed to the funding acquisition, and writing - review and editing. RK contributed to the funding acquisition, and writing - review and editing. AFAJ contributed to the conceptualization, methodology, supervision, funding acquisition, and writing - review and editing.

Competing interests. The authors declare that they have no conflict of interest.

Acknowledgements. This work is supported by a NASA HiMAT2 grant (#NNH19ZDA001N-HMA). HiMAT2 is an interdisciplinary multi-investigator effort to understand the cryospheric and hydrological state of HMA. We also acknowledge the National Center for Atmospheric Research (NCAR) (sponsored by the National Science Foundation (NSF)) for assisting this ongoing study. This work is in tandem with the goals of the Aerosol subgroup under HiMAT2, to quantify the deposition of aerosols over snow in HMA. We would also like to thank Miguel Hilario and Debottama Das for discussions about this work.



References

- 760 Andreae, M. O. and Rosenfeld, D.: Aerosol–cloud–precipitation interactions. Part 1. The nature and sources of cloud-active aerosols, *Earth-Science Reviews*, 89, 13–41, 2008.
- Archer-Nicholls, S., Lowe, D., Schultz, D. M., and McFiggans, G.: Aerosol–radiation–cloud interactions in a regional coupled model: the effects of convective parameterisation and resolution, *Atmospheric Chemistry and Physics*, 16, 5573–5594, 2016.
- Barnett, T. P., Adam, J. C., and Lettenmaier, D. P.: Potential Impacts of a Warming Climate on Water Availability in Snow-Dominated
765 Regions, *Nature*, 438, 303–309, <https://doi.org/10.1038/nature04141>, 2005.
- Barthlott, C., Zarbo, A., Matsunobu, T., and Keil, C.: Impacts of combined microphysical and land-surface uncertainties on convective clouds and precipitation in different weather regimes, *Atmospheric Chemistry and Physics*, 22, 10 841–10 860, 2022.
- Bergstra, J., Komer, B., Eliasmith, C., Yamins, D., and Cox, D. D.: Hyperopt: a Python library for model selection and hyperparameter optimization, *Comput. Sci. Discov.*, 8, 014 008, 2015.
- 770 Bickel, P. J., Götze, F., and van Zwet, W. R.: *Resampling Fewer Than n Observations: Gains, Losses, and Remedies for Losses*, Springer, New York, NY, https://doi.org/10.1007/978-1-4614-1314-1_17, 2012.
- Bocquet, M. et al.: Data assimilation in atmospheric chemistry models: current status and future prospects for coupled chemistry meteorology models, *Atmospheric Chemistry and Physics*, 15, 5325–5358, 2015.
- Bonekamp, P. N. J., de Kok, R. J., Collier, E., and Immerzeel, W. W.: Contrasting Meteorological Drivers of the Glacier Mass Balance
775 Between the Karakoram and Central Himalaya, *Frontiers in Earth Science*, 7, 2019.
- Bonekamp, P. N. J., Wanders, N., van der Wiel, K., Lutz, A. F., and Immerzeel, W. W.: Using large ensemble modelling to derive future changes in mountain specific climate indicators in a 2 and 3°C warmer world in High Mountain Asia, *International Journal of Climatology*, 41, E964–E979, 2021.
- Bony, S., Stevens, B., Frierson, D. M. W., Jakob, C., Kageyama, M., Pincus, R., Shepherd, T. G., Sherwood, S. C., Siebesma,
780 A. P., Sobel, A. H., Watanabe, M., and Webb, M. J.: Clouds, circulation and climate sensitivity, *Nature Geoscience*, 8, 261–268, <https://doi.org/10.1038/ngeo2398>, 2015.
- Borys, R. D., Lowenthal, D. H., and Mitchell, D. L.: The relationships among cloud microphysics, chemistry, and precipitation rate in cold mountain clouds, *Atmospheric Environment*, 34, 2593–2602, 2000.
- Brown, H. et al.: Brown Carbon Fuel and Emission Source Attributions to Global Snow Darkening Effect, *Journal of Advances in Modeling
785 Earth Systems*, 14, e2021MS002 768, 2022.
- Carlsaw, K. S. et al.: Large contribution of natural aerosols to uncertainty in indirect forcing, *Nature*, 503, 67–71, 2013.
- Castelvecchi, D.: Can we open the black box of AI?, *Nature News*, 538, 20, 2016.
- Cervený, R. S. and Balling Jr., R. C.: The impact of snow cover on diurnal temperature range, *Geophysical Research Letters*, 19, 797–800, 1992.
- 790 Chen, T. and Guestrin, C.: XGBoost: A Scalable Tree Boosting System, *Association for Computing Machinery*, <https://doi.org/10.1145/2939672.2939785>, 2016.
- Christidis, N. and Stott, P. A.: Changes in the Geopotential Height at 500 hPa under the Influence of External Climatic Forcings, *Geophysical Research Letters*, 42, 10,798–10,806, <https://doi.org/10.1002/2015GL066669>, 2015.
- Cohen, J. and Entekhabi, D.: The influence of snow cover on northern hemisphere climate variability, *Atmosphere-Ocean*, 39, 35–53, 2001.



- 795 Crumley, R. L., Palomaki, R. T., Nolin, A. W., Sproles, E. A., and Mar, E. J.: SnowCloudMetrics: Snow Information for Everyone, Remote Sensing, 12, 3341, <https://doi.org/10.3390/rs12203341>, 2020.
- Dagan, G., Yehekel, N., and Williams, A. I. L.: Radiative forcing from aerosol–cloud interactions enhanced by large-scale circulation adjustments, *Nature Geoscience*, 16, 1092–1098, <https://doi.org/10.1038/s41561-023-01319-8>, 2023.
- Danielson, J. J. and Gesch, D. B.: Global Multi-Resolution Terrain Elevation Data 2010 (GMTED2010), 2011.
- 800 Das, S. et al.: Linkage between the absorbing aerosol-induced snow darkening effects over the Himalayas-Tibetan Plateau and the pre-monsoon climate over northern India, *Theor Appl Climatol*, 147, 1033–1048, 2022.
- Duan, A. and Wu, G.: Change of cloud amount and the climate warming on the Tibetan Plateau, *Geophysical Research Letters*, 33, 2006.
- Fan, J., Rosenfeld, D., Ding, Y., Leung, L. R., and Li, Z.: Potential aerosol indirect effects on atmospheric circulation and radiative forcing through deep convection, *Geophysical Research Letters*, 39, <https://doi.org/10.1029/2012GL051851>, <https://onlinelibrary.wiley.com/doi/pdf/10.1029/2012GL051851>, 2012.
- 805 Feingold, G. et al.: New approaches to quantifying aerosol influence on the cloud radiative effect, *Proceedings of the National Academy of Sciences*, 113, 5812–5819, 2016.
- Fernandes, R., Zhao, H., Wang, X., Key, J., Qu, X., and Hall, A.: Controls on Northern Hemisphere Snow Albedo Feedback Quantified Using Satellite Earth Observations, *Geophysical Research Letters*, 36, <https://doi.org/10.1029/2009GL040057>, 2009.
- 810 Flanner, M. G., Zender, C. S., Randerson, J. T., and Rasch, P. J.: Present-day climate forcing and response from black carbon in snow, *Journal of Geophysical Research: Atmospheres*, 112, 2007.
- Flanner, M. G., Shell, K. M., Barlage, M., Perovich, D. K., and Tschudi, M. A.: Radiative forcing and albedo feedback from the Northern Hemisphere cryosphere between 1979 and 2008, *Nature Geoscience*, 4, 151–155, 2011.
- Flanner, M. G. et al.: SNICAR-ADv3: a community tool for modeling spectral snow albedo, *Geoscientific Model Development*, 14, 7673–7704, 2021.
- 815 Flato, G. M.: Earth System Models: An Overview, *WIREs Climate Change*, 2, 783–800, <https://doi.org/10.1002/wcc.148>, 2011.
- Gautam, R., Hsu, N. C., Lau, W. K.-M., and Yasunari, T. J.: Satellite observations of desert dust-induced Himalayan snow darkening, *Geophysical Research Letters*, 40, 988–993, 2013.
- Gelaro, R. et al.: The Modern-Era Retrospective Analysis for Research and Applications, Version 2 (MERRA-2), *Journal of Climate*, 30, 820 5419–5454, 2017.
- Gettelman, A.: Putting the clouds back in aerosol–cloud interactions, *Atmospheric Chemistry and Physics*, 15, 12 397–12 411, 2015.
- Gillett, N. P., Fyfe, J. C., and Parker, D. E.: Attribution of Observed Sea Level Pressure Trends to Greenhouse Gas, Aerosol, and Ozone Changes, *Geophysical Research Letters*, 40, 2302–2306, <https://doi.org/10.1002/grl.50500>, 2013.
- Giorgi, F. and Gao, X.-J.: Regional earth system modeling: review and future directions, *Atmospheric and Oceanic Science Letters*, 11, 825 189–197, <https://doi.org/10.1080/16742834.2018.1452520>, 2018.
- Gregory, J. M., Ingram, W. J., Palmer, M. A., Jones, G. S., Stott, P. A., Thorpe, R. B., Lowe, J. A., Johns, T. C., and Williams, K. D.: A New Method for Diagnosing Radiative Forcing and Climate Sensitivity, *Geophysical Research Letters*, 31, <https://doi.org/10.1029/2003GL018747>, 2004.
- Gryspeerdt, E. et al.: Wet scavenging limits the detection of aerosol effects on precipitation, *Atmospheric Chemistry and Physics*, 15, 7557–7570, 2015.
- 830 Hall, D. K. and Riggs, G. A.: MODIS/Aqua Snow Cover Daily L3 Global 0.05Deg CMG, Version 61, <https://doi.org/10.5067/MODIS/MYD10C1.061>, 2021a.



- Hall, D. K. and Riggs, G. A.: MODIS/Terra Snow Cover Daily L3 Global 0.05Deg CMG, Version 61, <https://doi.org/10.5067/MODIS/MOD10C1.061>, 2021b.
- 835 Hao, D. et al.: A parameterization of sub-grid topographical effects on solar radiation in the E3SM Land Model (version 1.0): implementation and evaluation over the Tibetan Plateau, *Geoscientific Model Development*, 14, 6273–6289, 2021.
- Harder, P., Pomeroy, J. W., and Helgason, W.: Local-Scale Advection of Sensible and Latent Heat During Snowmelt, *Geophysical Research Letters*, 44, 9769–9777, <https://doi.org/10.1002/2017GL074394>, 2017.
- Harte, J.: Toward a Synthesis of the Newtonian and Darwinian Worldviews, *Physics Today*, 55, 29–34, 2002.
- 840 He, C.: Modelling light-absorbing particle–snow–radiation interactions and impacts on snow albedo: fundamentals, recent advances and future directions, *Environmental Chemistry*, 19, 296–311, 2022.
- He, C. et al.: Black carbon-induced snow albedo reduction over the Tibetan Plateau: uncertainties from snow grain shape and aerosol–snow mixing state based on an updated SNICAR model, *Atmospheric Chemistry and Physics*, 18, 11 507–11 527, 2018.
- Heinze, C., Eyring, V., Friedlingstein, P., Jones, C., Balkanski, Y., Collins, W., Fichet, T., Gao, S., Hall, A., Ivanova, D., et al.: ESD
- 845 Reviews: Climate feedbacks in the Earth system and prospects for their evaluation, *Earth System Dynamics*, 10, 379–452, 2019.
- Hersbach, H. et al.: The ERA5 global reanalysis, *Quarterly Journal of the Royal Meteorological Society*, 146, 1999–2049, 2020.
- Hileman, B.: Web of interactions makes it difficult to untangle global warming data, *Chemical and Engineering News*; (United States), 70, 1992.
- Holtslag, A. a. M., Svensson, G., Baas, P., Basu, S., Beare, B., Beljaars, A. C. M., Bosveld, F. C., Cuxart, J., Lindvall, J., Steeneveld, G. J., Tjernström, M., and Wiel, B. J. H. V. D.: Stable Atmospheric Boundary Layers and Diurnal Cycles: Challenges for Weather
- 850 and Climate Models, *Bulletin of the American Meteorological Society*, 94, 1691–1706, <https://doi.org/10.1175/BAMS-D-11-00187.1>, publisher: American Meteorological Society Section: Bulletin of the American Meteorological Society, 2013.
- Hu, Y., Yu, H., Kang, S., Yang, J., Rai, M., Yin, X., Chen, X., and Chen, P.: Aerosol–meteorology feedback diminishes the transboundary transport of black carbon into the Tibetan Plateau, *Atmospheric Chemistry and Physics*, 24, 85–107, [https://doi.org/10.5194/acp-24-85-](https://doi.org/10.5194/acp-24-85-2024)
- 855 2024, publisher: Copernicus GmbH, 2024.
- Huang, H., Qian, Y., He, C., Bair, E. H., and Rittger, K.: Snow Albedo Feedbacks Enhance Snow Impurity-Induced Radiative Forcing in the Sierra Nevada, *Geophysical Research Letters*, 49, e2022GL098 102, 2022.
- Huffman, G. J. et al.: GPM IMERG Final Precipitation L3 1 day 0.1 degree x 0.1 degree V06, <https://doi.org/10.5067/GPM/IMERGDF/DAY/06>, 2014.
- 860 Inglis, A., Parnell, A., and Hurley, C. B.: Visualizing Variable Importance and Variable Interaction Effects in Machine Learning Models, *Journal of Computational and Graphical Statistics*, 31, 766–778, 2022.
- Inness, A. et al.: The CAMS reanalysis of atmospheric composition, *Atmospheric Chemistry and Physics*, 19, 3515–3556, 2019.
- Jiang, R., Tang, W., Wu, X., and Fu, W.: A random forest approach to the detection of epistatic interactions in case-control studies, *BMC Bioinformatics*, 10, S65, 2009.
- 865 Jiang, X. et al.: Impacts of ENSO and IOD on Snow Depth Over the Tibetan Plateau: Roles of Convections Over the Western North Pacific and Indian Ocean, *Journal of Geophysical Research: Atmospheres*, 124, 11 961–11 975, 2019.
- Jin, M. and Dickinson, R. E.: Land surface skin temperature climatology: benefitting from the strengths of satellite observations, *Environmental Research Letters*, 5, 044 004, 2010.
- Johnson, J. S. et al.: Evaluating uncertainty in convective cloud microphysics using statistical emulation, *Journal of Advances in Modeling*
- 870 Earth Systems, 7, 162–187, 2015.



- Kang, S., Zhang, Y., Qian, Y., and Wang, H.: A review of black carbon in snow and ice and its impact on the cryosphere, *Earth-Science Reviews*, 210, 103346, 2020.
- Kapnick, S. B., Delworth, T. L., Ashfaq, M., Malyshev, S., and Milly, P. C. D.: Snowfall less sensitive to warming in Karakoram than in Himalayas due to a unique seasonal cycle, *Nature Geoscience*, 7, 834–840, 2014.
- 875 Kraaijenbrink, P. D. A., Stigter, E. E., Yao, T., and Immerzeel, W. W.: Climate change decisive for Asia's snow meltwater supply, *Nature Climate Change*, 11, 591–597, 2021.
- Kraskov, A., Stögbauer, H., and Grassberger, P.: Estimating mutual information, *Phys. Rev. E*, 69, 066138, 2004.
- Krinner, G., Derksen, C., Essery, R., Flanner, M., Hagemann, S., Clark, M., Hall, A., Rott, H., Brutel-Vuilmet, C., Kim, H., Ménard, C. B., Mudryk, L., Thackeray, C., Wang, L., Arduini, G., Balsamo, G., Bartlett, P., Boike, J., Boone, A., Chéruy, F., Colin, J., Cuntz, M., Dai, 880 Y., Decharme, B., Derry, J., Ducharme, A., Dutra, E., Fang, X., Fierz, C., Ghattas, J., Gusev, Y., Haverd, V., Kontu, A., Lafaysse, M., Law, R., Lawrence, D., Li, W., Marke, T., Marks, D., Ménégoz, M., Nasonova, O., Nitta, T., Niwano, M., Pomeroy, J., Raleigh, M. S., Schaedler, G., Semenov, V., Smirnova, T. G., Stacke, T., Strasser, U., Svenson, S., Turkov, D., Wang, T., Wever, N., Yuan, H., Zhou, W., and Zhu, D.: ESM-SnowMIP: assessing snow models and quantifying snow-related climate feedbacks, *Geoscientific Model Development*, 11, 5027–5049, <https://doi.org/10.5194/gmd-11-5027-2018>, publisher: Copernicus GmbH, 2018.
- 885 Kumar, R., Barth, M. C., Pfister, G. G., Naja, M., and Brasseur, G. P.: WRF-Chem simulations of a typical pre-monsoon dust storm in northern India: influences on aerosol optical properties and radiation budget, *Atmospheric Chemistry and Physics*, 14, 2431–2446, 2014.
- Kumar, R., He, C., Roychoudhury, C., Cheng, W., Mizukami, N., and Arellano, A. F.: High Mountain Asia 12 km Modeled Estimates of Aerosol Transport, Chemistry, and Deposition Reanalysis, 2003–2019, Version 1, Boulder, Colorado USA. NASA National Snow and Ice Data Center Distributed Active Archive Center, <https://doi.org/10.5067/CG4OT8DJX2Z7>, [Data Set], 2024.
- 890 Kumar, R. et al.: Influences of the springtime northern Indian biomass burning over the central Himalayas, *Journal of Geophysical Research: Atmospheres*, 116, 2011.
- Lam, R., Sanchez-Gonzalez, A., Willson, M., Wirnsberger, P., Fortunato, M., Alet, F., Ravuri, S., Ewalds, T., Eaton-Rosen, Z., Hu, W., Merose, A., Hoyer, S., Holland, G., Vinyals, O., Stott, J., Pritzel, A., Mohamed, S., and Battaglia, P.: Learning skillful medium-range global weather forecasting, *Science*, 382, 1416–1421, <https://doi.org/10.1126/science.adi2336>, 2023.
- 895 Lau, K. M., Kim, M. K., and Kim, K. M.: Asian summer monsoon anomalies induced by aerosol direct forcing: the role of the Tibetan Plateau, *Clim Dyn*, 26, 855–864, 2006.
- Lau, W. K. M. and Kim, K.-M.: Impact of Snow Darkening by Deposition of Light-Absorbing Aerosols on Snow Cover in the Himalayas–Tibetan Plateau and Influence on the Asian Summer Monsoon: A Possible Mechanism for the Blanford Hypothesis, *Atmosphere*, 9, 438, 2018.
- 900 Lauer, A., Eyring, V., Bellprat, O., Bock, L., Gier, B. K., Hunter, A., Lorenz, R., Pérez-Zanón, N., Righi, M., Schlund, M., Senfleben, D., Weigel, K., and Zechlau, S.: Earth System Model Evaluation Tool (ESMValTool) v2.0 – Diagnostics for Emergent Constraints and Future Projections from Earth System Models in CMIP, *Geoscientific Model Development*, 13, 4205–4228, <https://doi.org/10.5194/gmd-13-4205-2020>, 2020.
- Lee, J., Gleckler, P. J., Ahn, M.-S., Ordonez, A., Ullrich, P. A., Sperber, K. R., Taylor, K. E., Planton, Y. Y., Guilyardi, E., Durack, P., Bonfils, 905 C., Zelinka, M. D., Chao, L.-W., Dong, B., Doutriaux, C., Zhang, C., Vo, T., Boutte, J., Wehner, M. F., Pendergrass, A. G., Kim, D., Xue, Z., Wittenberg, A. T., and Krasting, J.: Systematic and Objective Evaluation of Earth System Models: PCMDI Metrics Package (PMP) Version 3, *Geoscientific Model Development*, 17, 3919–3948, <https://doi.org/10.5194/gmd-17-3919-2024>, 2024.



- Lee, L. A. et al.: The magnitude and causes of uncertainty in global model simulations of cloud condensation nuclei, *Atmospheric Chemistry and Physics*, 13, 8879–8914, 2013.
- 910 Li, Z., Lau, W. K.-M., Ramanathan, V., Wu, G., Ding, Y., Manoj, M. G., Liu, J., Qian, Y., Li, J., Zhou, T., Fan, J., Rosenfeld, D., Ming, Y., Wang, Y., Huang, J., Wang, B., Xu, X., Lee, S.-S., Cribb, M., Zhang, F., Yang, X., Zhao, C., Takemura, T., Wang, K., Xia, X., Yin, Y., Zhang, H., Guo, J., Zhai, P. M., Sugimoto, N., Babu, S. S., and Brasseur, G. P.: Aerosol and monsoon climate interactions over Asia, *Reviews of Geophysics*, 54, 866–929, <https://doi.org/10.1002/2015RG000500>, _eprint: <https://onlinelibrary.wiley.com/doi/pdf/10.1002/2015RG000500>, 2016.
- 915 Lipton, Z. C.: The Mythos of Model Interpretability: In machine learning, the concept of interpretability is both important and slippery, *Queue*, 16, 31–57, 2018.
- Liu, Y. and Margulis, S. A.: High mountain asia UCLA daily snow reanalysis, version 1, <https://doi.org/10.5067/HNAUGJQXSCVU>, 2021.
- Liu, Y., Fang, Y., and Margulis, S. A.: Spatiotemporal distribution of seasonal snow water equivalent in High Mountain Asia from an 18-year Landsat–MODIS era snow reanalysis dataset, *The Cryosphere*, 15, 5261–5280, 2021a.
- 920 Liu, Y., Li, Z., and Chen, Y.: Continuous warming shift greening towards browning in the Southeast and Northwest High Mountain Asia, *Scientific Reports*, 11, 17920, 2021b.
- Liu, Y. et al.: Biophysical impacts of vegetation dynamics largely contribute to climate mitigation in High Mountain Asia, *Agricultural and Forest Meteorology*, 327, 109233, 2022.
- Lohmann, U.: Anthropogenic Aerosol Influences on Mixed-Phase Clouds, *Current Climate Change Reports*, 3, 32–44, 2017.
- 925 Lohmann, U. and Feichter, J.: Global indirect aerosol effects: a review, *Atmospheric Chemistry and Physics*, 5, 715–737, 2005.
- Lundberg, S. M. et al.: From local explanations to global understanding with explainable AI for trees, *Nat Mach Intell*, 2, 56–67, 2020.
- Lyapustin, A.: MODIS/Terra+Aqua AOD and Water Vapor from MAIAC, Daily L3 Global 0.05Deg CMG V061, <https://doi.org/10.5067/MODIS/MCD19A2CMG.061>, 2023.
- Maina, F. Z., Kumar, S. V., Albergel, C., and Mahanama, S. P.: Warming, increase in precipitation, and irrigation enhance greening in High Mountain Asia, *Communications Earth Environment*, 3, 1–8, 2022.
- 930 Meehl, G. A., S. T. F. C. W. D. F. P. G. A. T. G. J. M. K. A. K. R. M. J. M. N. A. R. S. C. W. I. G. W. A. J. and Zhao, Z. C.: Global climate projections. Chapter 10, 2007.
- Michibata, T., Suzuki, K., and Takemura, T.: Snow-induced buffering in aerosol–cloud interactions, *Atmospheric Chemistry and Physics*, 20, 13771–13780, <https://doi.org/10.5194/acp-20-13771-2020>, publisher: Copernicus GmbH, 2020.
- 935 Ming, Y. and Ramaswamy, V.: A Model Investigation of Aerosol-Induced Changes in Tropical Circulation, *Journal of Climate*, <https://doi.org/10.1175/2011JCLI4108.1>, 2011.
- Mlawer, E. J., Taubman, S. J., Brown, P. D., Iacono, M. J., and Clough, S. A.: Radiative transfer for inhomogeneous atmospheres: RRTM, a validated correlated-k model for the longwave, *Journal of Geophysical Research: Atmospheres*, 102, 16663–16682, 1997.
- Moch, J. M. et al.: Aerosol-Radiation Interactions in China in Winter: Competing Effects of Reduced Shortwave Radiation and Cloud-Snowfall-Albedo Feedbacks Under Rapidly Changing Emissions, *Journal of Geophysical Research: Atmospheres*, 127, e2021JD035442, 2022.
- 940 Mudryk, L. et al.: Historical Northern Hemisphere snow cover trends and projected changes in the CMIP6 multi-model ensemble, *The Cryosphere*, 14, 2495–2514, 2020.
- Mülmenstädt, J. and Wilcox, L. J.: The Fall and Rise of the Global Climate Model, *Journal of Advances in Modeling Earth Systems*, 13, e2021MS002781, <https://doi.org/10.1029/2021MS002781>, 2021.
- 945



- Muñoz-Sabater, J. et al.: ERA5-Land: a state-of-the-art global reanalysis dataset for land applications, *Earth System Science Data*, 13, 4349–4383, 2021.
- National Academies of Sciences, Engineering, and Medicine: Next Generation Earth Systems Science at the National Science Foundation, The National Academies Press, Washington, DC, <https://doi.org/10.17226/26042>, 2022.
- 950 National Academies Press: Thriving on Our Changing Planet: A Decadal Strategy for Earth Observation from Space, National Academies Press, Washington, D.C., <https://doi.org/10.17226/24938>, 2018.
- Newman, M. E. J.: Assortative Mixing in Networks, *Physical Review Letters*, 89, 208 701, <https://doi.org/10.1103/PhysRevLett.89.208701>, publisher: American Physical Society, 2002.
- NOAA Science Advisory Board: A Report on Priorities for Weather Research, https://sab.noaa.gov/wp-content/uploads/2021/12/PWR-Report_Final_12-9-21.pdf, 119, 2021.
- 955 Nobre, C., Brasseur, G. P., Shapiro, M. A., Lahten, M., Brunet, G., Busalacchi, A. J., Hibbard, K., Seitzinger, S., Noone, K., and Ometto, J. P.: Addressing the Complexity of the Earth System, *Bulletin of the American Meteorological Society*, <https://doi.org/10.1175/2010BAMS3012.1>, 2010.
- Ohmura, A., Kasser, P., and Funk, M.: Climate at the Equilibrium Line of Glaciers, *Journal of Glaciology*, 38, 397–411, 1992.
- 960 Oleson, K. W. et al.: Technical description of version 4.0 of the community land model (CLM), NCAR Tech. Note NCAR/TN-478+ STR, 257, 1–257, 2010.
- Orsolini, Y. et al.: Evaluation of snow depth and snow cover over the Tibetan Plateau in global reanalyses using in situ and satellite remote sensing observations, *The Cryosphere*, 13, 2221–2239, 2019.
- Painter, T. H. et al.: Impact of disturbed desert soils on duration of mountain snow cover, *Geophysical Research Letters*, 34, 2007.
- 965 Pepin, N. et al.: Elevation-dependent warming in mountain regions of the world, *Nature Climate Change*, 5, 424–430, 2015.
- Qian, Y. et al.: Light-absorbing particles in snow and ice: Measurement and modeling of climatic and hydrological impact, *Advances in Atmospheric Sciences*, 32, 64–91, 2015.
- Qu, X. and Hall, A.: What Controls the Strength of Snow-Albedo Feedback?, *Journal of Climate*, <https://doi.org/10.1175/JCLI4186.1>, 2007.
- Ragettli, S., Immerzeel, W. W., and Pellicciotti, F.: Contrasting climate change impact on river flows from high-altitude catchments in the Himalayan and Andes Mountains, *Proceedings of the National Academy of Sciences*, 113, 9222–9227, 2016.
- 970 Rahimi, S., Liu, X., Zhao, C., Lu, Z., and Lebo, Z. J.: Examining the Atmospheric Radiative and Snow-Darkening Effects of Black Carbon and Dust across the Rocky Mountains of the United States Using WRF-Chem, *Atmospheric Chemistry and Physics*, 20, 10 911–10 935, <https://doi.org/10.5194/acp-20-10911-2020>, 2020.
- Ramanathan, V. et al.: Atmospheric brown clouds: Hemispherical and regional variations in long-range transport, absorption, and radiative forcing, *Journal of Geophysical Research: Atmospheres*, 112, 2007.
- 975 Randles, C. A. et al.: The MERRA-2 Aerosol Reanalysis, 1980 Onward. Part I: System Description and Data Assimilation Evaluation, *Journal of Climate*, 30, 6823–6850, 2017.
- Reichstein, M., Camps-Valls, G., Stevens, B., Jung, M., Denzler, J., Carvalhais, N., and Prabhat: Deep Learning and Process Understanding for Data-Driven Earth System Science, *Nature*, 566, 195–204, <https://doi.org/10.1038/s41586-019-0912-1>, 2019.
- 980 RGI Consortium, .: Randolph Glacier Inventory - A Dataset of Global Glacier Outlines, Version 6, <https://doi.org/10.7265/4m1f-gd79>, 2017.
- Ripple, W. J., Wolf, C., Lenton, T. M., Gregg, J. W., Natali, S. M., Duffy, P. B., Rockström, J., and Schellnhuber, H. J.: Many risky feedback loops amplify the need for climate action, *One Earth*, 6, 86–91, 2023.



- Rittger, K., Bormann, K. J., Bair, E. H., Dozier, J., and Painter, T. H.: Evaluation of VIIRS and MODIS Snow Cover Fraction in High-Mountain Asia Using Landsat 8 OLI, *Frontiers in Remote Sensing*, 2, 2021.
- 985 Robock, A.: Ice and Snow Feedbacks and the Latitudinal and Seasonal Distribution of Climate Sensitivity, *Journal of the Atmospheric Sciences*, 40, 986–997, 1983.
- Roychoudhury, C., He, C., Kumar, R., McKinnon, J. M., and Arellano Jr., A. F.: On the Relevance of Aerosols to Snow Cover Variability Over High Mountain Asia, *Geophysical Research Letters*, 49, e2022GL099317, 2022.
- Sakai, A. and Fujita, K.: Contrasting glacier responses to recent climate change in high-mountain Asia, *Scientific Reports*, 7, 13717, 2017.
- 990 Sand, M., Samset, B. H., Tsigaridis, K., Bauer, S. E., and Myhre, G.: Black Carbon and Precipitation: An Energetics Perspective, *Journal of Geophysical Research: Atmospheres*, 125, e2019JD032239, 2020.
- Sand, M., Samset, B. H., Myhre, G., Glib, J., Bauer, S. E., Bian, H., Chin, M., Checa-Garcia, R., Ginoux, P., Kipling, Z., Kirkevåg, A., Kokkola, H., Le Sager, P., Lund, M. T., Matsui, H., van Noije, T., Olivieri, D. J. L., Remy, S., Schulz, M., Stier, P., Stjern, C. W., Takemura, T., Tsigaridis, K., Tsyro, S. G., and Watson-Parris, D.: Aerosol Absorption in Global Models from AeroCom Phase III, *Atmospheric*
- 995 *Chemistry and Physics*, 21, 15929–15947, <https://doi.org/10.5194/acp-21-15929-2021>, 2021.
- Sandu, I., van Niekerk, A., Shepherd, T. G., Vosper, S. B., Zadra, A., Bacmeister, J., Beljaars, A., Brown, A. R., Dörnbrack, A., McFarlane, N., Pithan, F., and Svensson, G.: Impacts of orography on large-scale atmospheric circulation, *npj Climate and Atmospheric Science*, 2, 1–8, <https://doi.org/10.1038/s41612-019-0065-9>, publisher: Nature Publishing Group, 2019.
- Sarangi, C. et al.: Dust dominates high-altitude snow darkening and melt over high-mountain Asia, *Nature Climate Change*, 10, 1045–1051,
- 1000 2020.
- Schlögl, S., Lehning, M., and Mott, R.: How Are Turbulent Sensible Heat Fluxes and Snow Melt Rates Affected by a Changing Snow Cover Fraction?, *Frontiers in Earth Science*, 6, <https://doi.org/10.3389/feart.2018.00154>, publisher: Frontiers, 2018.
- Schneider, T., Lan, S., Stuart, A., and Teixeira, J.: Earth System Modeling 2.0: A Blueprint for Models That Learn From Observations and Targeted High-Resolution Simulations, *Geophysical Research Letters*, 44, 12396–12417, <https://doi.org/10.1002/2017GL076101>,
- 1005 [_eprint: https://onlinelibrary.wiley.com/doi/pdf/10.1002/2017GL076101](https://onlinelibrary.wiley.com/doi/pdf/10.1002/2017GL076101), 2017.
- Senf, F., Quaas, J., and Tegen, I.: Absorbing aerosol decreases cloud cover in cloud-resolving simulations over Germany, *Quarterly Journal of the Royal Meteorological Society*, 147, 4083–4100, <https://doi.org/10.1002/qj.4169>, [_eprint: https://onlinelibrary.wiley.com/doi/pdf/10.1002/qj.4169](https://onlinelibrary.wiley.com/doi/pdf/10.1002/qj.4169), 2021.
- Shepherd, T. G.: Atmospheric circulation as a source of uncertainty in climate change projections, *Nature Geoscience*, 7, 703–708,
- 1010 <https://doi.org/10.1038/ngeo2253>, publisher: Nature Publishing Group, 2014.
- Shi, X., Groisman, P. Y., Déry, S. J., and Lettenmaier, D. P.: The role of surface energy fluxes in pan-Arctic snow cover changes, *Environmental Research Letters*, 6, 035204, <https://doi.org/10.1088/1748-9326/6/3/035204>, 2011.
- Shi, X., Déry, S. J., Groisman, P. Y., and Lettenmaier, D. P.: Relationships between Recent Pan-Arctic Snow Cover and Hydroclimate Trends, *Journal of Climate*, 26, 2048–2064, 2013.
- 1015 Shi, Z. et al.: Snow-darkening versus direct radiative effects of mineral dust aerosol on the Indian summer monsoon onset: role of temperature change over dust sources, *Atmospheric Chemistry and Physics*, 19, 1605–1622, 2019.
- Shin, N.-Y., Ham, Y.-G., Kim, J.-H., Cho, M., and Kug, J.-S.: Application of Deep Learning to Understanding ENSO Dynamics, *Artificial Intelligence for the Earth Systems*, <https://doi.org/10.1175/AIES-D-21-0011.1>, 2022.
- Shindell, D. and Faluvegi, G.: Climate response to regional radiative forcing during the twentieth century, *Nature Geoscience*, 2, 294–300,
- 1020 2009.



- Singh, D., Zhu, Y., Liu, S., Srivastava, P. K., Dharpure, J. K., Chatterjee, D., Sahu, R., and Gagnon, A. S.: Exploring the Links between Variations in Snow Cover Area and Climatic Variables in a Himalayan Catchment Using Earth Observations and CMIP6 Climate Change Scenarios, *Journal of Hydrology*, 608, 127–148, <https://doi.org/10.1016/j.jhydrol.2022.127648>, 2022.
- Skamarock, W. C., Klemp, J. B., Dudhia, J., Gill, D. O., Barker, D. M., Duda, M. G., Huang, X.-Y., Wang, W., and Powers, J. G.: A Description of the Advanced Research WRF Version 3, NCAR Tech. Note., <https://doi.org/10.5065/D68S4MVH>, 2008.
- 1025 Soden, B. J., Held, I. M., Colman, R., Shell, K. M., Kiehl, J. T., and Shields, C. A.: Quantifying Climate Feedbacks Using Radiative Kernels, *Journal of Climate*, 21, 3504–3520, <https://doi.org/10.1175/2007JCLI2110.1>, publisher: American Meteorological Society Section: *Journal of Climate*, 2008.
- Sorg, A., Stoffel, M., Solomina, O., and Beniston, M.: Climate change impacts on glaciers and runoff in Tien Shan (Central Asia), *Nature* 1030 *Climate Change*, 2, 725–731, 2012.
- Stainforth, D. A., Aina, T., Christensen, C., Collins, M., Faull, N., Frame, D. J., Kettleborough, J. A., Knight, S., Martin, A., Murphy, J. M., Piani, C., Sexton, D., Smith, L. A., Spicer, R. A., Thorpe, A. J., and Allen, M. R.: Uncertainty in predictions of the climate response to rising levels of greenhouse gases, *Nature*, 433, 403–406, <https://doi.org/10.1038/nature03301>, publisher: Nature Publishing Group, 2005.
- Stein, U. and Alpert, P.: Factor Separation in Numerical Simulations, *Journal of Atmospheric Sciences*, 50, 2107–2115, 1993.
- 1035 Stevens, B. and Bony, S.: What Are Climate Models Missing?, *Science*, 340, 1053–1054, <https://doi.org/10.1126/science.1237554>, publisher: American Association for the Advancement of Science, 2013.
- Stevens, B. and Feingold, G.: Untangling aerosol effects on clouds and precipitation in a buffered system, *Nature*, 461, 607–613, 2009.
- Södergren, A. H., McDonald, A. J., and Bodeker, G. E.: An energy balance model exploration of the impacts of interactions between surface albedo, cloud cover and water vapor on polar amplification, *Climatic Dynamics*, 51, 1639–1658, 2018.
- 1040 Tonidandel, S. and LeBreton, J. M.: Relative importance analysis: A useful supplement to regression analysis, *Journal of Business and Psychology*, 26, 1–9, 2011.
- Tuccella, P., Pitari, G., Colaiuda, V., Raparelli, E., and Curci, G.: Present-Day Radiative Effect from Radiation-Absorbing Aerosols in Snow, *Atmospheric Chemistry and Physics*, 21, 6875–6893, <https://doi.org/10.5194/acp-21-6875-2021>, 2021.
- Usha, K. H., Nair, V. S., and Babu, S. S.: Modeling of aerosol induced snow albedo feedbacks over the Himalayas and its implications on regional climate, *Climate Dynamics*, 54, 4191–4210, 2020.
- 1045 van Vuuren, D. P., Bayer, L. B., Chuwah, C., Ganzeveld, L., Hazeleger, W., van den Hurk, B., van Noije, T., O'Neill, B., and Strengers, B. J.: A Comprehensive View on Climate Change: Coupling of Earth System and Integrated Assessment Models, *Environmental Research Letters*, 7, 024012, <https://doi.org/10.1088/1748-9326/7/2/024012>, 2012.
- Wall, C. J. et al.: Assessing effective radiative forcing from aerosol–cloud interactions over the global ocean, *Proceedings of the National Academy of Sciences*, 119, e2210481 119, 2022.
- 1050 Wan, Z., Hook, S., and Hulley, G.: MOD11C1 MODIS/Terra Land Surface Temperature/Emissivity Daily L3 Global 0.05Deg CMG V006, <https://doi.org/10.5067/MODIS/MOD11C1.006>, 2015a.
- Wan, Z., Hook, S., and Hulley, G.: MYD11C1 MODIS/Aqua Land Surface Temperature/Emissivity Daily L3 Global 0.05Deg CMG V006, <https://doi.org/10.5067/MODIS/MYD11C1.006>, 2015b.
- 1055 Wang, P., Yang, Y., Xue, D., Ren, L., Tang, J., Leung, L. R., and Liao, H.: Aerosols Overtake Greenhouse Gases Causing a Warmer Climate and More Weather Extremes toward Carbon Neutrality, *Nature Communications*, 14, 7257, <https://doi.org/10.1038/s41467-023-42891-2>, 2023.



- Wang, W., Huang, X., Deng, J., Xie, H., and Liang, T.: Spatio-Temporal Change of Snow Cover and Its Response to Climate over the Tibetan Plateau Based on an Improved Daily Cloud-Free Snow Cover Product, *Remote Sensing*, 7, 169–194, 2015.
- 1060 Warren, S. G. and Wiscombe, W. J.: A Model for the Spectral Albedo of Snow. II: Snow Containing Atmospheric Aerosols, *Journal of the Atmospheric Sciences*, 1980.
- Wood Jr, F. B.: The Need for Systems Research on Global Climate Change, *Systems Research*, 5, 225–240, <https://doi.org/10.1002/sres.3850050305>, 1988.
- World Meteorological Organization (WMO): The 2022 GCOS ECVs Requirements (GCOS 245), GCOS Rep. 245, 12 pp. [Available online
1065 at <https://library.wmo.int/records/item/58111-the-2022-gcos-ecvs-requirements-gcos-245>], 2022.
- Wu, X., Naegeli, K., Premier, V., Marin, C., Ma, D., Wang, J., and Wunderle, S.: Evaluation of Snow Extent Time Series Derived from Advanced Very High Resolution Radiometer Global Area Coverage Data (1982–2018) in the Hindu Kush Himalayas, *The Cryosphere*, 15, 4261–4279, <https://doi.org/10.5194/tc-15-4261-2021>, 2021.
- Xiao, Y., Ke, C.-Q., Shen, X., Cai, Y., and Li, H.: What drives the decrease of glacier surface albedo in High Mountain Asia in the past two
1070 decades?, *Science of The Total Environment*, 863, 160 945, 2023.
- Yao, T., Xue, Y., Chen, D., Chen, F., Thompson, L., Cui, P., Koike, T., Lau, W. K.-M., Lettenmaier, D., Mosbrugger, V., Zhang, R., Xu, B., Dozier, J., Gillespie, T., Gu, Y., Kang, S., Piao, S., Sugimoto, S., Ueno, K., Wang, L., Wang, W., Zhang, F., Sheng, Y., Guo, W., Ailikun, Yang, X., Ma, Y., Shen, S. S. P., Su, Z., Chen, F., Liang, S., Liu, Y., Singh, V. P., Yang, K., Yang, D., Zhao, X., Qian, Y., Zhang, Y., and Li, Q.: Recent Third Pole’s Rapid Warming Accompanies Cryospheric Melt and Water Cycle Intensification and Interactions
1075 between Monsoon and Environment: Multidisciplinary Approach with Observations, Modeling, and Analysis, *Bulletin of the American Meteorological Society*, <https://doi.org/10.1175/BAMS-D-17-0057.1>, 2019.
- You, Q. et al.: Review of snow cover variation over the Tibetan Plateau and its influence on the broad climate system, *Earth-Science Reviews*, 201, 103 043, 2020.
- Zhang, F., Thapa, S., Immerzeel, W., Zhang, H., and Lutz, A.: Water availability on the Third Pole: A review, *Water Security*, 7, 100 033,
1080 <https://doi.org/https://doi.org/10.1016/j.wasec.2019.100033>, 2019.
- Zhou, M. et al.: The impact of aerosol–radiation interactions on the effectiveness of emission control measures, *Environmental Research Letters*, 14, 024 002, 2019.

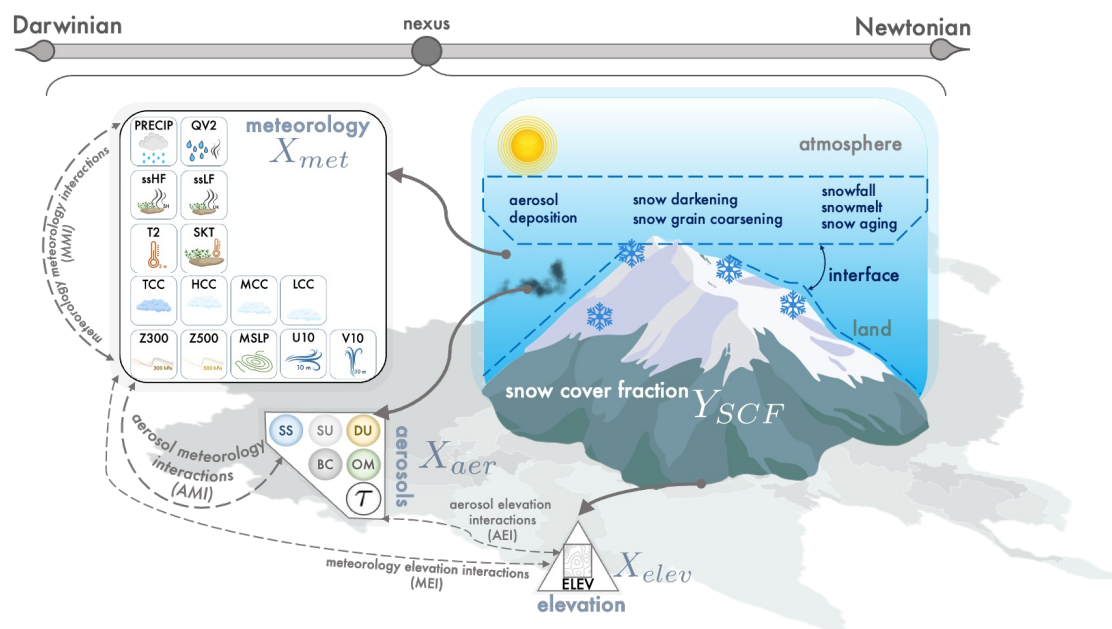


Figure 1. Schematic describing an integrated approach to assess interactions at the atmospheric-cryospheric (land) interface over High Mountain Asia. The Darwinian view focuses on the individual predictors (shown by the 22 icons grouped by meteorology, aerosols, and elevation) that drive snowmelt while the Newtonian view emphasizes emerging patterns and physics-based processes driving snowmelt (shown in the interface between the atmosphere and land). This study lies at the nexus of both perspectives where we assess the sensitivity of snow cover fraction to the interactions between aerosols and meteorology variables at the interface (aerosol-meteorology interactions or AMI) on snow. Likewise, we also consider meteorology-meteorology interactions (MMI) on snow, aerosol–elevation interactions onto snow (AEI), and meteorology–elevation interactions (MEI) on snow. The overlaid map of Asia is taken from FreeVectorMaps at <https://freevectormaps.com/world-maps/asia/WRLD-AS-02-4001?ref=atr>.

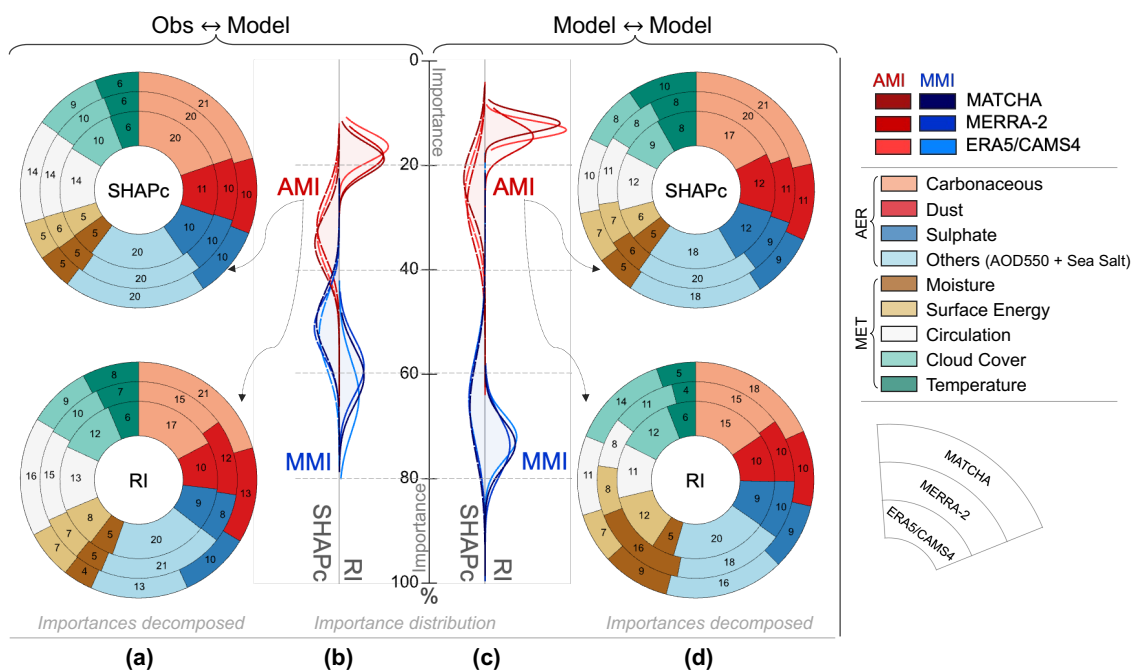


Figure 2. Importance of aerosol-meteorology interactions on snow and their constituent variables. Distributions of importance metrics (b-c), relative importance (RI), and Shapely contribution (SHAPc) for aerosol-meteorology (AMI) and meteorology-meteorology (MMI) interactions on snow shown for the Obs-Model (b) and Model-Model (c) construct for the three reanalyses. AMI’s importance on snow is further decomposed into nine subgroups of predictors (four aerosol/AER and five meteorology/MET subgroups), which are shown in the donut pie-plots for the Obs-Model (a) and Model-Model (d) constructs for both RI (bottom row) and SHAPc (top row). The innermost ring shows the contribution of each subgroup to AMI’s importance on snow from the ERA5-CAMS4 reanalysis, followed by MERRA-2 and MATCHA in the outermost ring.

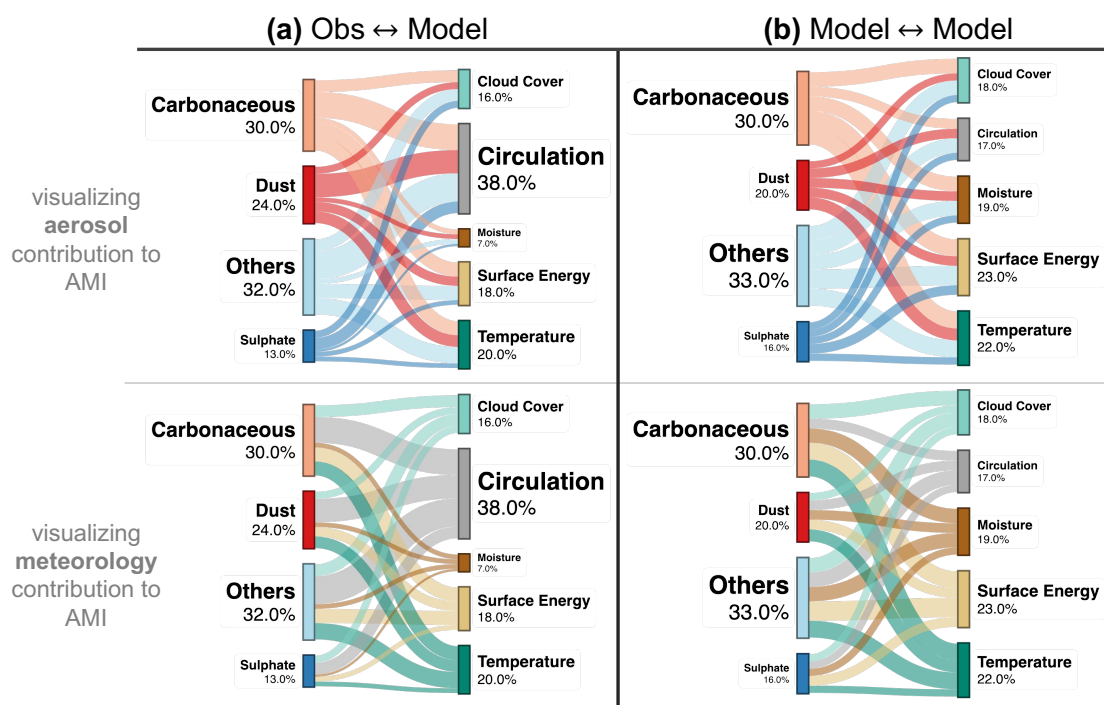


Figure 3. Importance of different aerosol and meteorology groups to AMI on snow for both constructs across all three reanalyses. Flow diagrams depicting the sum of the contribution of four aerosol groups and five meteorology groups to AMI in low snow-cover regions during the late snowmelt period (May-July) across the Obs-Model (a) and Model-Model construct (b), similar to the donut plots in Fig. 2(a) and 2(d), except the contribution is aggregated for all three reanalyses and both importance metrics. The top row shows the contributions color-coded by aerosol groups, and the bottom row shows the same contributions color-coded by meteorology groups. The flow diagrams are made using SankeyMATIC.

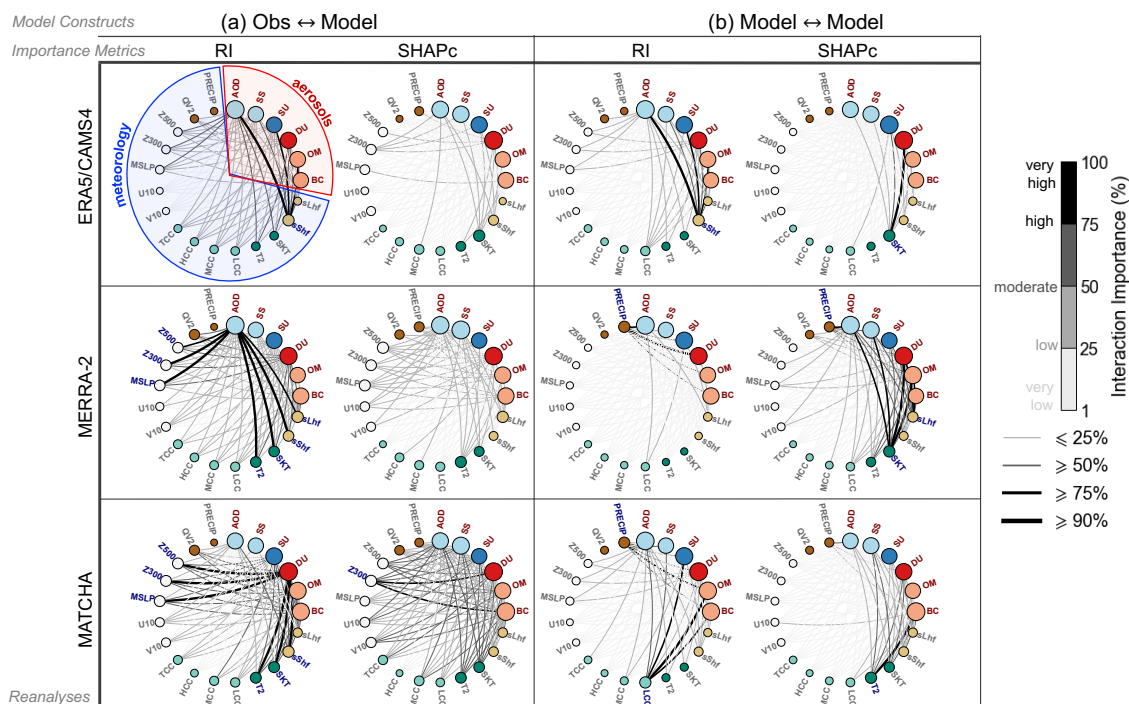


Figure 4. Strength of aerosol-meteorology interactions on snow within each reanalysis for different metrics and constructs. Network diagrams depicting the interaction importance/strength for both model constructs, Obs-Model (a) and Model-Model (b) using the relative importance (RI) and Shapely contribution (SHAPc) importance metrics of predictors within aerosol-meteorology interactions onto snow (AMI) in low snow-cover regions during the late snowmelt period (May-July). The nodes denote each predictor, while the lines (edges) denote the interaction importance on snow between the aerosol and meteorology variables, with their weights denoting the strength of the importance (1 to 100%, very low-low for $\leq 25\%$, low-moderate for 25% to 50%, moderate-high for 50% to 75%, and high-very high for $\geq 75\%$ shown in the color bars). The node sizes differ between AER and MET predictors based on their weighted degree (number of edge connections, see Appendix A). The variable abbreviations at the nodes include the following aerosol variables; AOD for total AOD at 550 nm; SU for surface sulphate mixing ratio; SS for surface sea-salt mixing ratio; DU for surface dust mixing ratio; OM for surface organic matter mixing ratio and BC for surface black carbon mixing ratio. For meteorology, the abbreviations are as follows, PRECIP for daily accumulated precipitation; QV2 for specific humidity at 2 m; Z500 and Z300 for geopotential height at 500 and 300 hPa; U10 and V10 for zonal and meridional winds at 10 m; MSLP for mean sea level pressure; MCC, TCC, LCC and HCC for medium, total, low and high cloud cover fraction; T2 for temperature at 2 m; SKT for skin temperature; sShf and sLhf for surface sensible and latent heat flux; and finally ELEV for elevation. Details about these predictors can be found in Supplementary Table 2.

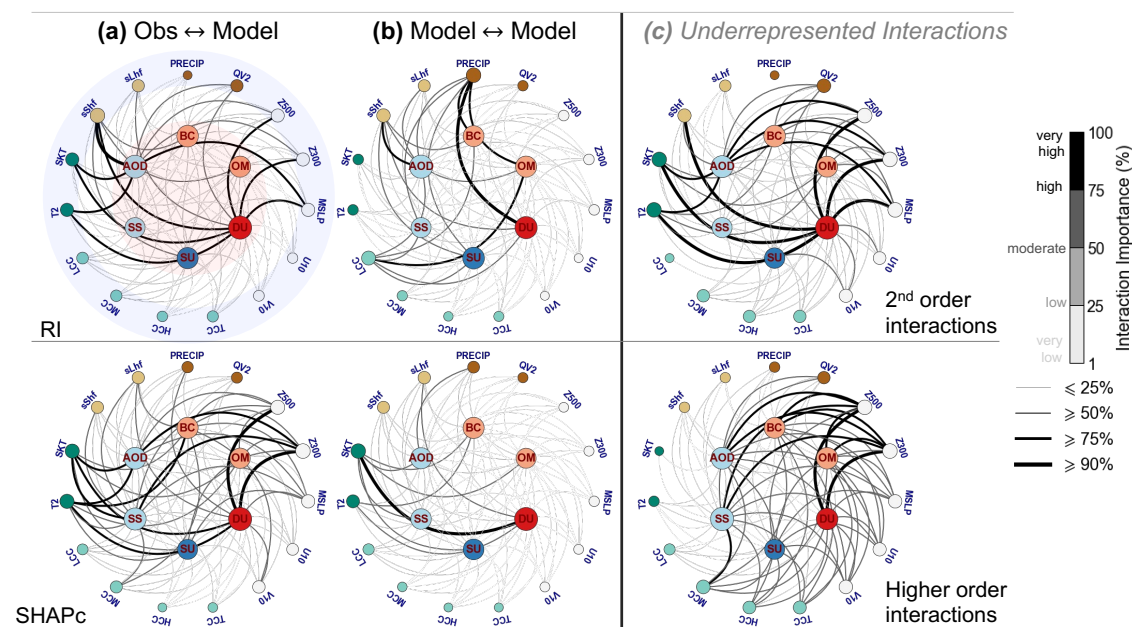


Figure 5. Major aerosol-meteorology interactions at the snow interface for different importance metrics and constructs for all three reanalyses. Network diagrams depicting the interactions aggregated across all three reanalyses (a-b) for each construct and importance metric (RI and SHAPc). Networks in (c) show underrepresented interactions captured by RI and SHAPc that should be emphasized across all three reanalyses. The nodes are arranged in a concentric fashion, with innermost nodes representing aerosol predictors (highlighted in red in the first network from top left) and the outermost nodes representing meteorology predictors (highlighted in blue in the first network from top left). The interaction importances are shown through edge connections between the nodes and are weighted by colors and width denoting the strength of the importance (1 to 100%, very low-low for $\leq 25\%$, low-moderate for 25% to 50%, moderate-high for 50% to 75%, and high-very high for $\geq 75\%$ shown in the color bar).

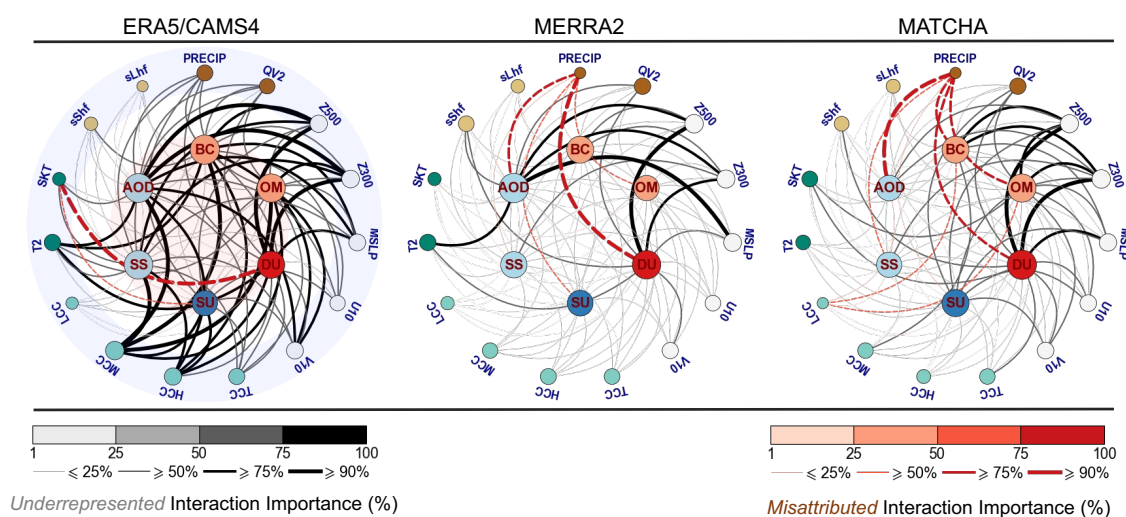


Figure 6. Underrepresented and misattributed aerosol-meteorology interactions on snow in each reanalysis. Network diagrams depicting the underrepresented and misattributed interaction importance/strength in AMI on snow across all three reanalyses. These are estimated using the difference in the interactions between the Obs-Model and Model-Model construct for each reanalysis. The positive differences shown by black edge connections highlight underrepresented interactions, while the negative difference shown by red edge (dashed) connections highlight misattributed interactions. The differences in the importance of these interactions (both positive and negative) are normalized separately (1 to 100%) for relative comparison. The nodes are arranged in a concentric fashion, with innermost nodes representing aerosol predictors (highlighted in red in the first network from left) and the outermost nodes representing meteorology predictors (highlighted in blue in the first network from left).

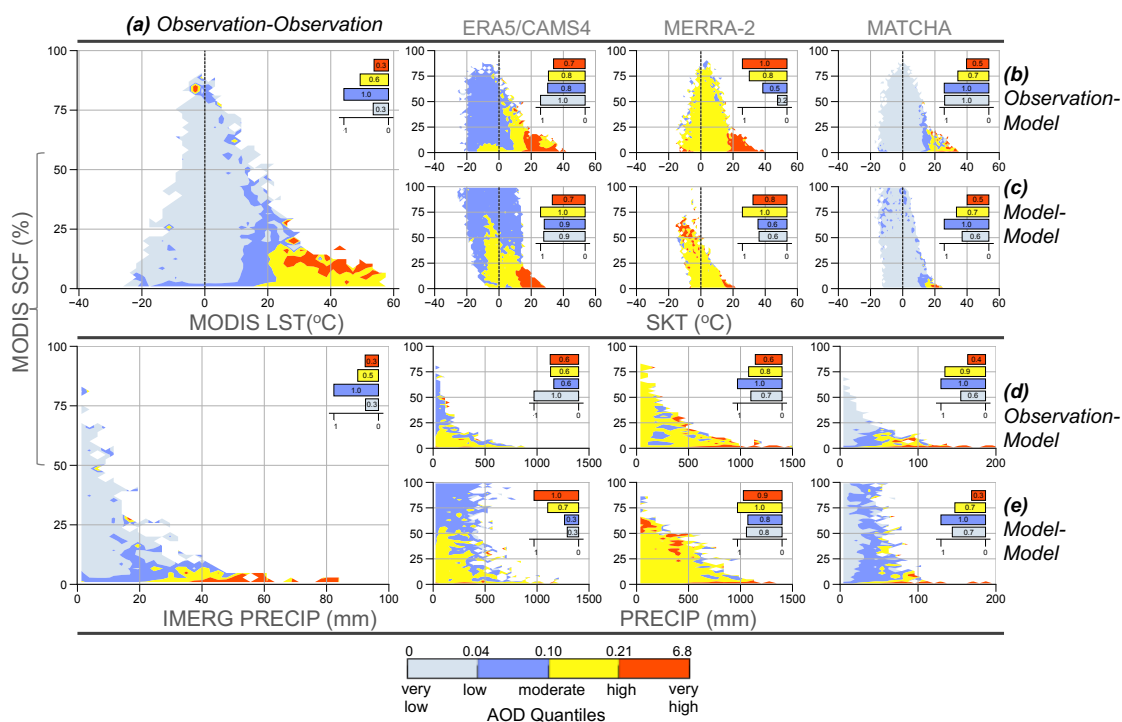


Figure 7. Relationships between aerosols and meteorology to snow cover fraction in low snow-covered regions across all three constructs. Scatter density of AOD at 550 nm based on snow cover fraction (SCF) in the y-axis with land surface temperature/skin temperature (LST/SKT) (top row) and daily accumulated precipitation (PRECIP) (bottom row) in the x-axes across the Obs-Obs construct (a), Obs-Model construct (b,d) and Model-Model construct (c,e). The variables are of daily resolution and masked for the low snow-covered regions. The scatter densities are classified (colored) by quantiles of AOD at 550 nm (shown in the legend) based on the respective aerosol datasets across the three constructs (MAIAC AOD for Obs-Obs, reanalysis AOD for the other two). The color bar represents the quantiles of AOD at 550 nm from very low to very high (0th, 25th, 50th, 75th, and 100th percentiles), computed across all three constructs (Obs-Obs, Obs-Mod, and the Mod-Mod construct). The bar graphs denote the non-linear sensitivity (quantified by max-normalized mutual information between 0 and 1) of SCF to LST/SKT and PRECIP at various quantiles of AOD for relative comparison of the sensitivity across different AOD quantiles.



Table 1. Statistics of the importance of AMI (in %) across all three reanalyses, two constructs and two importance metrics.

Reanalysis	Construct		Obs-Model		Model-Model			
			RI		SHAPc			
	μ	σ	μ	σ	μ	σ	μ	σ
ERA5/CAMS4	16.6	2.8	33.7	6.3	13.4	1.7	25.3	6.8
MERRA-2	18.2	3.2	31.6	6.1	14.7	2.9	27.8	7.6
MATCHA	19.0	3.1	35.1	5.6	12.2	1.8	22.8	6.4

Table 2. Dissortativity for the individual networks in Fig. 4. Dissortativity values lie between 0 and -1.

Reanalysis	Dissortativity			
	Construct		Model-Model	
	Obs-Model	SHAP	RI	SHAP
ERA5/CAMS4	-0.7	-0.7	-0.6	-0.4
MERRA-2	-0.5	-0.8	-0.4	-0.7
MATCHA	-0.6	-0.9	-0.7	-0.6